Leptin resistance establishment in the ovary of diet-induced obese mice and its relationship with cumulus cells transcriptome

Karolina Wołodko[1], Edyta Walewska[1], Juan Castillo-Fernandez[2], Gavin Kelsey[2,3,*], António Galvão[1,2,3,*]

[1] *Institute of Animal Reproduction and Food Research of PAS, Olsztyn, Poland;*

[2] *Epigenetics Programme, Babraham Institute, Cambridge, CB22 3AT, UK;*

[3] *Centre for Trophoblast Research, University of Cambridge, Cambridge, CB2 3EG, UK.*

Keywords: obesity, ovary, cumulus cells, leptin, SOC33, transcriptome

---

[*]Corresponding author:

António Galvão

Antonio.Galvao@babraham.ac.uk
Epigenetics Programme, Babraham Institute, Cambridge, CB22 3AT, UK
a.galvao@pan.olsztyn.pl
Institute of Animal Reproduction and Food Research of PAS, Olsztyn, Poland

Gavin Kelsey

Gavin.Kelsey@babraham.ac.uk
Epigenetics Programme, Babraham Institute, Cambridge, CB22 3AT, UK

ABSTRACT

Obesity is associated with infertility, decreased ovarian performance and lipotoxicity. Nonetheless, little is known about the aetiology of these reproductive impairments. Here, we investigated the extent of which leptin signalling is altered in the ovary upon obesity, with particular emphasis on effects on cumulus cells (CCs), the intimate functional companions of the oocyte. Using diet-induced obesity (DIO) (4 and 16wks) and pharmacological hyperleptinemic (LEPT) mouse models, we discovered that obesity leads to ovarian leptin resistance after 16wk high fat diet (HFD), as evidenced by increases in the feedback regulator SOCS3 and decreases in the positive effectors pJAK2 and ObRb-pTyr985. Transcriptome analysis of CCs revealed a complex response to DIO, with large numbers and distinct sets of genes deregulated at early and late stages of obesity. Transcriptome analysis indicated an overlap between LEPT and 4wk HFD treatment in the upregulation of glucose metabolism, and downregulation of cytoskeleton organisation. Whereas after 16wk HFD CCs showed augmented inflammatory responses and cell morphogenesis, and decreased metabolism and transport. Amongst the differentially expressed genes at late stage, we noted a striking correlation with body weight. Generally, obesity leads to ovarian leptin resistance and major temporal changes in gene expression regulation in CCs.

INTRODUCTION

Obesity is considered one of the major public health challenges of modern times and has been linked to various comorbidities, such as metabolic syndrome, type 2 diabetes, cancer, stroke (Schelbert, 2009) and infertility (Pasquali, Patton, & Gambineri, 2007). Obese women have an increased risk of menstrual dysfunctions and anovulation, pregnancy complications, and poor reproductive outcome (Dağ & Dilbaz, 2015). In mouse models, obesity is characterised by lipid accumulation in the ovary and ensuing lipotoxicity (Unger & Zhou, 2001) and oxidative stress (Robker, Wu, & Yang, 2011). Nonetheless, the exact mechanisms underlying ovarian pathogenesis in the course of obesity remain uncharacterised.

Leptin is a cytokine mainly secreted by the adipose tissue (adipokine) in large amounts during obesity (Friedman & Halaas, 1998; Maffei et al., 1995). Leptin controls food intake through its action at the central nervous system (Vaisse et al., 1996); however, as a pleiotropic cytokine, leptin contributes to the regulation of numerous processes in the body, such as the immune response (Cava & Matarese, 2004), angiogenesis (Sierra-Honigmann et al., 1998), or insulin-mediated events in the liver (Szanto & Kahn, 2000). Concerning the reproductive tract, leptin was shown to control the neuroendrocrine reproductive axis (Louis et al., 2011, Quennell et al., 2009) and folliculogenesis (Panwar, Herrid, Kauter, & McFarlane, 2012). Furthermore, leptin has been linked to ovulation (L. Dupuis et al., 2013) and embryo development (Herrid, Nguyen, Hinch, & McFarlane, 2006). Leptin is detected in most cell types in the murine ovary, with the highest staining seen in the oocyte (Ryan et al., 2002). The leptin receptor b (ObRb) is a type I cytokine receptor, which signals through association with the tyrosine kinase Janus kinase 2 (JAK2). Upon leptin binding and dimerization of the receptor, JAK2 is recruited (Kloek et al., 2002), mediating the phosphorylation of three conserved tyrosine residues on the intracellular domain of the receptor: tyrosine (Tyr) 985, Tyr1077 and Tyr1138. Subsequently, signalling molecules are recruited to these activated tyrosines (Banks, Davis, Bates, & Myers, 2000; Gong et al., 2007). As a consequence, the signal transducer and activator of transcription

(STAT) 5 and/or STAT3 are also phosphorylated and translocated to the nucleus, where they regulate transcription (Mütze, Roth, Gerstberger, & Hübschle, 2007; Vaisse et al., 1996). During sustained activation of ObRb, the expression of the suppressor of cytokine signalling 3 (SOCS3) and tyrosine-protein phosphatase 1B (PTP1B) is initiated as a negative feedback response (Bjørbæk et al., 2000; Zabolotny et al., 2002). While PTP1B dephosphorylates JAK2, SOCS3 binds to receptor domains within JAK2 and Tyr985 and terminates signal transduction.

To date, little is known about the integrity of leptin signalling in the ovary during obesity progression, and its particular impact on the cumulus oophorous complex (COC). Here, we demonstrate the establishment of leptin resistance in the ovary of obese mice during diet-induced obesity (DIO), inferring also that early SOCS3 activation can block JAK2 and STAT5 phosphorylation. Furthermore, we reveal the asynchronous response of different ovarian components to increased ObRb activation, substantiating the higher sensitivity of cumulus cells (CCs). Transcriptome analysis of CCs isolated from super-ovulated COCs reveals the changes in gene expression signatures across time. The initial changes, after 4 weeks (wk) DIO, in cell trafficking and metabolism, are followed by mounting inflammation and cell reorganisation at 16 wk DIO. We also characterise the particular role of altered leptin signalling in those events, leading to the perturbation of cell trafficking and membrane transport, as well as metabolism. These datasets represent a powerful reference in assisted reproduction techniques in humans, in which sampling the oocyte is uncommon but CCs are frequently available for analysis.

RESULTS

1. Leptin signalling is impaired in the whole ovary of diet-induced obese mice

Initially we sought to characterise changes in leptin signalling in the ovary throughout diet-induced obesity. Thus, mice were subjected to high fat diet (HFD) for 4 and 16 wk and ovaries were collected for mRNA and protein analysis. DIO mice significantly gained body weight (BW) and fat mass (FM) already at 4 wk, with an average absolute gain in BW of 13

grams (g) in the 16 wk HFD group (Figure 1- figure supplement 1A, $p<0.05$). Importantly, we excluded from 16 wk HFD animals below 33 g of BW. Also, we confirmed establishment of glucose intolerance and insulin resistance at 16 wk HFD (Figure 1- figure supplement 1F, 1G, $p<0.05$). Furthermore, we monitored the oestrous cycle, finding that the 4 wk HFD group had higher prevalence of oestrus counts compared with CD controls, whereas in the 16 wk HFD group there was a reduction in pro-oestrus (Figure 1- figure supplement 1H, 1I, $p<0.05$). Whole ovaries were then used to determine expression of the leptin receptor and components of leptin signalling by real-time PCR, including mRNAs for the leptin receptor short and long isoforms (*ObR*, *ObRb*), and the downstream components *Jak2*, *Sh2 domain-containing protein 1b (Sh2b)*, *Stat3*, *Stat5a*, *Stat5b*, *Ptp1b*, and *Socs3* (primers in supplementary file 1 Table 1). We found that *Stat5a* expression was decreased after 4 wk HFD (Figure 1E, $p<0.05$), whereas *Stat3*, *Ptp1b* and *Socs3* were increased (Figure 1D, Figure 1- figure supplement 2D, figure 1F; $p<0.05$, $p<0.05$, $p<0.01$ respectively). In parallel, we assessed protein levels of ObR and ObRb and phosphorylation of ObRb on Tyr 985, 1077 and 1138 by Western blotting. We also measured phosphorylation of downstream activators of the leptin receptor JAK2, STAT3 and STAT5, together with the expression of the inhibitors PTP1B and SOCS3. At 4 wk HFD we observed increased levels of pTyr985 ObRb (Figure 1B, $p<0.05$) and SOCS3 (Figure 1F, $p<0.05$), but a reduction in pSTAT5 (Figure 1E, $p<0.01$). After 16 wk HFD, the short form ObR (Figure 1A, $p<0.01$), as well as pJAK2 and pSTAT5 were decreased compared to control (Figure 1C, 1E, $p<0.05$, $p<0.01$ respectively). Additionally, SOCS3 protein was upregulated at the same time point (Figure 1F, $p<0.001$), but no changes were found in PTP1B protein level (Figure 1- figure supplement 2D). This is suggestive of impaired leptin signalling in the ovary after 16 wk HFD. The increased SOCS3 and decreased abundance of pTyr985 and pJAK2 were strong evidence for the establishment of leptin resistance after 16 wk HFD.

2. An in vivo mouse model of pharmacological hyperleptinemia

After identifying the major molecular changes in leptin signalling in the ovaries of DIO females, we aimed to establish an *in vivo* system that would expose ovaries to the systemic levels of leptin seen in obese mice, but in the absence of the remaining traits of obesity. Thus, we conceived a model for pharmacological hyperleptinemia (LEPT), in which female mice were injected 100 μg/day with leptin for 9 and 16 days (d). The phenotype and cyclicity of this model were characterised, revealing a consistent drop in BW and FM after 9- and 16 d (Figure 2- figure supplement 1A, 1D; $p<0.05$) and increased incidence of oestrus in LEPT (Figure 2- figure supplement 1F; $p<0.05$). The ovaries were collected for mRNA and protein analysis of the same markers previously assessed in the DIO experiment. The first timepoint indicated a consistent decrease in transcript abundance of *Obrb, Stat3, Ptp1b* (Figure 2A, 2D, Figure 2- figure supplement 2C; $p<0.05$ respectively) and *Socs3* (Figure 2F; $p<0.001$), compared to control. Conversely, after 16 d LEPT, there was an increase in transcripts for *Jak2 and Socs3* (Figure 2C, 2F; $p<0.05$). Concerning protein expression, after 16 d LEPT a reduction in ObR and pSTAT5 (Figure 2A, 2E; $p<0.05$, $p<0.01$ respectively) levels was observed simultaneously with the upregulation of SOCS3 (Figure 2F; $p<0.05$). We also confirmed upregulation of SOCS3 in the ovaries of DIO and LEPT by enzyme-linked immunosorbent assay (ELISA), despite decreased leptin measured in 16 d LEPT (Figure 2- figure supplement 3, $p<0.05$), which was related with lack specificity of kit towards the recombinant leptin administered. Finally, other phenotypic assessments were the increased plasma levels of leptin and insulin at both time-points of the DIO protocol (Figure 2- figure supplement 3B and 3C; $p<0.01$), but no changes in the LEPT protocol, and no changes in adiponectin in either model (Figure 2- figure supplement 3A). Validation of a pharmacological hyperleptinemic model allowed us to access ovarian samples from mice with hyperactivation of ObRb, here indicated by increased SOCS3 expression, but lacking all the remaining traits of obesity.

3. Responses of different ovarian compartments to leptin signalling

Next, we sought to characterise the extent to which various ovarian components responded differently to increased circulating leptin. The results above suggested that SOCS3 could be an important player in establishment of leptin resistance in the ovary of obese mice. Thus, we examined SOCS3 protein in ovaries of DIO, LEPT and the genetically obese model: mice with a mutation in the obese (*ob*) gene, on the C57BL/6J background (B6.Cg-Lep^{ob}/J - *ob/ob)*. Immunohistochemistry (IHC) revealed expression of SOCS3 in oocytes from primordial, primary, secondary and antral follicles (Figure 3B-F, respectively); in addition, stromal compartment enriched in theca cells (TC) and granulosa cells (GC) from the respective follicles were stained, as well as the ovarian stroma (Figure 3D-F). Importantly, we compared the IHC staining of SOCS3 and PTP1B in 16 wk HFD ovaries, which suggested that SOCS3 is the major ObRb inhibitor being expressed in the oocyte and granulosa cells, as PTP1B protein was not detected in the oocyte (Figure 3- figure supplement 1). As a control for the specificity of the IHC data, we used immunofluorescent (IF) confocal microscopy on sections from homozygous *ob/ob* (-/-) ovaries, observing a weaker intensity of SOCS3 in both oocyte and GC (Figure 3N, 3P) compared to wild type (+/+) (Figure 3M, 3O). These IF results confirmed the specificity of the staining, since SOCS3 is expected to be less abundant in the *ob/ob* mouse (Duan et al., 2007). Furthermore, we also inferred that impaired leptin signalling in the ovary is likely to have direct implications for the oocyte, since the gamete was shown to express SOCS3. Importantly, when we compared the transcription of leptin signalling mediators in whole ovary and TC, we found that *Socs3* mRNA was increased (Figure 3Q).

4. Cumulus cell transcriptome analysis: leptin versus diet induced obesity

Next, we analysed the transcriptome of CCs from LEPT, 4 wk DIO and 16 wk DIO protocols. For this analysis, we selected the 16 wk HFD group based on a BW of >35g, separated from the BWs of CD controls and from the 4 wk HFD group by at least 10g. After

superovulation, a total of 50-80 CCs were collected from each animal, from which RNA sequencing (RNA-seq) libraries were generated using a Smart-seq2 oligo-dT method (Picelli et al., 2013, 2014). Principal component analysis (PCA) of global gene expression did not show obvious clustering based on the dietary treatment, but revealed the proximity between the control for LEPT (CONT) and 4 wk chow diet (CD) group, which were age-matched control groups (Figure 4A). Furthermore, PC1 segregated LEPT samples, alongside two 16 wk CD samples (Figure 4A), which might suggest some heterogeneity in gene expression within the CD samples (see below). After DESeq2 analysis (false discovery rate - FDR <0.05), a total of 2,026 differently expressed genes (DEG) was found between LEPT and CONT samples (1,212 genes upregulated and 814 downregulated). With respect to DIO, we found 997 DEGs in 4 wk HFD (373 upregulated and 624 downregulated), and 846 DEGs in 16 wk HFD (203 upregulated and 643 downregulated; Figure 4C, 4D and 4E, respectively). Surprisingly, there were only 22 DEGs in common between the comparisons, 119 DEGs in common between LEPT and 4 wk HFD, whereas 312 DEGs were shared between LEPT and 16 wk HFD (Figure 4B). Finally, only 30 DEGs were commonly seen in 4 wk and 16 wk HFD (Figure 4B). Gene ontology (GO) (Eden, Lipson, Yogev, & Yakhini, 2007; Eden, Navon, Steinfeld, Lipson, & Yakhini, 2009) analysis of the DEG lists for each protocol showed that the upregulated genes for LEPT were associated primarily with cellular organisation and the cytoskeleton. Furthermore, the increase in transcripts involved in the immune response, such as *complement* (*C) 2*, *C4*, *toll-like receptor* (*Tlr)2* and *Tlr3*, supporting the immune-mediating role of leptin as evidenced before (Faggioni et al., 1998; Fantuzzi & Faggioni, 2000; Iikuni, Lam, Lu, Matarese, & La Cava, 2008). Importantly, the metabolic gene *Arachidonate 15-Lipoxygenase* (*Alox15)*, and the transcription factor *Hes Related Family BHLH Transcription Factor With YRPW Motif* (*Hey) 1*, were amongst the most significantly upregulated DEGs (Supplementary file 3 Table 3). The transcriptional repressor HEY1 is directly activated by Notch Receptor (NOTCH) 2 during follicular development, and both HEY1 and NOTCH2 were shown to be increased in

proliferating granulosa cells and can contribute to ovarian overstimulation and premature follicular failure (Vanorny & Mayo, 2017). Amongst the LEPT downregulated pathways we found several functions linked to cell metabolism, but also chromatin organisation and histone modifications (Figure 4- figure supplement 1A; Supplementary file 3 Table 3). With respect to 4 wk HFD, genes with increased transcription were primarily linked to nitrogen and lipid metabolism and transport, but also cell stress and reactive oxygen species generation (Supplementary file 4 Table 4). One of the most significantly increased transcripts was for *Argininosuccinate synthase (Ass) 1* (Supplementary file 4 Table 4) a gene involved in amino acid metabolism and mitochondrial function (Haines, Pendleton, & Eichler, 2011). Concerning downregulated genes after 4 wk HFD, we identified pathways involved in regulation of macromolecule biosynthesis and gene expression, as well as chromatin organisation/histone modification and regulation of cell cycle (Figure 4- figure supplement 1B; Supplementary file 4 Table 4). Finally, in the 16 wk HFD treatment, upregulated genes were associated with negative regulation of development and cellular component organisation (Figure 4- figure supplement 1C; Supplementary file 5 Table 5). The most increased gene was the *Guanylate-binding protein* (*Gbp*) *8* (Supplementary file 5 Table 5), a component of cellular response to interferon-gamma (Tripal et al., 2007). Conversely, the pathways highlighted for downregulated genes in 16 wk HFD were localisation, transport and positive regulation of metabolism (Figure 4- figure supplement 1C; Supplementary file 5 Table 5), and amongst the most inhibited genes we found the *Mediator of polymerase II RNA transcription (Med) 25*, which encodes a protein that is a key regulator of epigenetic mechanisms and plays a role in chromatin modification and Polycomb complex suppression (Englert, Luo, Goldstein, & Surapureddi, 2015) (Supplementary file 5 Table 5). Therefore, in this analysis we identified the gene signatures in CCs altered during the establishment and progression of obesity, as well as genes responsive to increased systemic levels of leptin.

5. Global transcriptome of CCs reflect the body weight of the mice

An unexpected observation from the previous experiment was the apparent heterogeneity seen in global transcriptome of the 16wk CD CCs (Figure 4A). We noted that there was a range in BW of the 16wk CD females; accordingly, we investigated whether transcriptional heterogeneity could be linked to the BW of the animals. We also analysed CCs from a group 16 wk HFD females with comparable food intake (FI) levels that exhibited less gain in BW (low gainers: HFDLG), and which had previously been excluded from the analysis on that basis. PCA of the three 16 wk groups CD, HFD and HFDLG suggested segregation of the samples in PC1 based on BW (Figure 5A). Furthermore, the correlation between PC1 and BW was r=0.777 (p=3.026e-06) (Figure 5B), which substantiates the physiological effect driven by BW, rather than the nature of the diet itself, on the global gene expression profile of CCs. Amongst the genes listed on the top of PC1 score, we found *Septin (Sept) 2*, required for the organisation of actin cytoskeleton (Kuo et al., 2015), or the transcription regulator *Med25* (Supplementary file 8 Table 8). Finally, when we evaluated expression of the 846 DEGs identified above from 16wk DIO with found that the 16wk HFDLG group exhibited an expression pattern closer to 16wk CD than to 16 wk HFD (Figure 5C). Thus, we find a strong correlation in the global gene expression profile in CC with BW, indicative of the strong impact of metabolism on ovarian function and CC physiology.

6. The contribution of leptin to changes in gene expression in CCs from obese mice

Next we investigated to what extent changes in gene expression in the ovary of obese mice could be ascribed to de-regulation of leptin signalling in CCs. Thus, we looked for the overlap between the DEG datasets from the LEPT, 4 wk, and 16 wk DIO groups. The rational for this analysis was to reveal major pathways regulated by leptin in these cells in the course of obesity. As a result, we found 144 genes upregulated in both LEPT and 4 wk HFD: these were related to response to toxins, transport and glucose metabolism (Figure 6A; Supplementary file

9 Table 9). More specifically, the genes *Lipocalin* (*Lcn*) *2, Annexin a11 (Anxa11)* and *Glucose-6-phosphate dehydrogenase x-linked* (*G6pdx*) were amongst the most significant ones (Figure 6A). Consistently, the GO terms associated with the 177 downregulated genes in both protocols were metabolism and gene expression regulation (Figure 6A; Supplementary file 9 Table 9). A number of downregulated genes were found to encode important epigenetic factors, such as *Dna segment, chr 14, abbott 1 expressed o* (*Tasor*), *Lysine (k)-specific methyltransferase 2d* (*Kmt2d*/*Mll2*), *Methyl-cpg binding domain protein* (*Mbd*) *2,* and *DNA methyltransferase* (*Dnmt*) *3a* (Figure 6B), which could indicate epigenetic dysregulation. Another important effect attributed to LEPT in early obesity was the inhibition of genes mediating actin-cytoskeleton reorganisation (Figure 6C; Supplementary file 9 Table 9). Indeed, cell trafficking and nutrient mobilisation to the oocyte, as well as the uptake of signalling molecules from the oocyte, is fundamental for COCs expansion and oocyte maturation (Russell, Gilchrist, Brown, & Thompson, 2016a). Furthermore, we assessed the potential impact of leptin on genes involved in CC metabolism, and verified the role of leptin on glucose metabolism (Figure 6D) and fatty acid oxidation (Figure 6E), which was reflected by the similarities between LEPT and 4 wk HFD. Here, we questioned how lack of leptin singling can be detrimental metabolically. For instance, the oocyte is unable to metabolise glucose due to low phosphofructokinase activity (Cetica, Pintos, Dalvit, & Beconi, 2002), highlighting the importance of CCs glycolytic activity in the generation of pyruvate (Thompson, Lane, & Gilchrist, 2007). This function appeared to be decreased in 16 wk HFD, which could be the result of the establishment of leptin resistance in the ovary. As a consequence, the transport of pyruvate into the oocyte would be decreased, which could directly impact the tricarboxylic acid cycle (TCA) and adenosine triphosphate (ATP) generation (Figure 6 – figure supplement 1B) (Sutton-McDowall, Gilchrist, & Thompson, 2010). Indeed, low ATP levels have been associated with low oocyte quality and early embryo development prognosis (Frank, Sutton-McDowall, Gilchrist, & Thompson, 2014; Jimenez et al., 2013). Leptin is also known to be key

for free fatty acid (FFA) metabolism, promoting their oxidation and regulating the homeostasis of triglycerides in a cell (Unger, Zhou, & Orci, 1999; Yamagishi et al., 2001). Thus, disruption of leptin signalling in 16 wk HFD CCs (Figure 6- figure supplement 1A) could be relevant for lipotoxicity and stress previously described in obese ovaries (Linda Lin-Yan Wu et al., 2010) (Figure 6- figure supplement 1E-F). Lastly, we investigated the gene-network interactions between leptin signalling genes and our group of DEGs from LEPT and 4 wk HFD. We identified 12 major clusters using community structure analysis (Figure 7A) (Gang Su, Kuchinsky, Morris, States, & Meng, 2010) (pairwise correlations > 0.90), with reference to the pathways revealed in Figure 7B (Supplementary file 10 Table 10). In general, leptin signalling hyperactivation in CCs seemed to be linked primarily to impaired cell membrane transport and endocytosis, but also cell metabolism and gene expression regulation.

7. Time span of events in CCs during obesity

In a final analysis, we characterised the changes in gene expression in CCs in early and late DIO. Using the average expression for CONT and 4 wk CD as timepoint 0 wk, we then considered the timepoints 4 wk and 16 wk of DIO. Initially, we identified 35 DEGs significantly downregulated (FDR < 0.05) in both 4 wk and 16 wk HFD (Figure 8A, Supplementary file 11 Table 11). The most significantly deregulated gene (FDR = 0.0002) at 4 wk HFD was *MICAL Like* (*Micall) 1*, which codes for a lipid-binding protein with high affinity for phosphatidic acid and is responsible for the regulation of membrane trafficking (Abou-Zeid et al., 2011). Accordingly, another gene inhibited during early obesity in CCs was *Dynein cytoplasmic 1 heavy chain* (*Dync1h*) *1*, involved in protein transport, positioning of cell compartments, and movement of structures within the cell (Vaisberg, Grissom, & McIntosh, 1996). These functions seem to be key for the complex homoeostasis of COCs, once the oocyte depends on metabolite transfer from CCs for nuclear maturation (Uyar, Torrealday, & Seli, 2013). At 16 wk, we also saw a strong inhibition of *Collagen* (*Col*) *6a3*, which binds

hyaluronan and other components of the extracellular matrix (ECM) (Adriaenssens, Mazoyer, Segers, Wathlet, & Smitz, 2009), and is responsive to epidermal growth factor (EGF) mediated CC expansion (Dunning et al., 2015). Thus, it is likely that exchanges between CCs and the oocyte could be affected already early in obesity, which poses major concerns for oocyte quality. Only three genes were significantly upregulated throughout DIO (Figure 8B), in particular the *retinoblastoma binding protein (Rbbp) 8*. Then, we looked up for genes with an opposing profile that could reflect dynamics of changes in the ovary in the course of obesity. Among the 10 genes upregulated at 4 wk and downregulated at 16 wk HFD we found *Annexin* (*Anxa) 11*, which is known to be involved in transmembrane secretion (Mirsaeidi, Gidfar, Vu, & Schraufnagel, 2016) (FDR<0.02, Figure 8C, Supplementary file 11 Table 11). Furthermore, the *Activating transcription factor 7-interacting protein* (*Atf7ip*) and *Exportin* (*Xpo*) *5*, known to mediate gene silencing (Supplementary file 11 Table 11), were also identified. Atf7ip is an important transcriptional regulator that can act either as an activator or a repressor, depending on the context, and was shown to be required for Human Silencing Hub (Hush)-mediated heterochromatin formation and gene silencing (Timms, Tchasovnikarova, Antrobus, Dougan, & Lehner, 2016). The contrasting gene signatures between 4- and 16 wk might suggest the cells try to adapt to a new physiological setting, but eventually fail with unusual genes being actively expressed. Finally, only 3 genes were inhibited at 4 wk and upregulated at 16 wk HFD (Supplementary file 11 Table 11). One was *Ras homology family member U* (*Rhou)* (Figure 8D), involved in the regulation of cell morphology (Tao, Pennica, Xu, Kalejta, & Levine, 2001). This is in line, again, with lipid dystrophy events previously discussed in the obese ovary (Linda L.-Y. Wu, Norman, & Robker, 2012). Finally, we identified the GOs shared between conditions, after plotting the DEG from 4 wk HFD against 16 wk HFD. Only 3 DEGs were upregulated in both conditions (Figure 8E). Concerning the 252 genes exclusively upregulated in 4 wk HFD, we had cell transport and localisation (Figure 8E; Supplementary file 11 Table 11), whereas the 30 genes upregulated in 16 wk HFD referred to immune

response (Figure 8E; Supplementary file 11 Table 11). Finally, a total of 694 DEGs were downregulated in both protocols, mainly linked to metabolism and transcription. Generally, this analysis revealed dramatic changes in gene expression in the ovary during obesity progression, identifying the chronology of molecular events occurring in CCs.

DISCUSSION

The present study characterises the molecular mechanisms underlying establishment of leptin resistance in the ovary of DIO mice. Furthermore, we validated a model with increased circulating levels of leptin – pharmacologically hyperleptinemic mouse – to pinpoint the exclusive effects of leptin-SOCS3 hyperactivation in the ovary. Finally, making use of sensitive methods for reduced-cell number RNA-seq, we studied the transcriptome of the somatic cells surrounding the oocyte from the groups LEPT, 4 wk and 16 wk DIO.

Leptin is a major adipokine that was initially linked to satiety (Friedman & Halaas, 1998). The establishment of leptin resistance at different levels in the body has been documented in recent years as one of the consequences of obesity (AHREN, 1999; Al Maskari & Alnaqdy, 2006). Accordingly, leptin signalling is deregulated in the hypothalamus (Bjørbaek & Kahn, 2004; Münzberg, Flier, & Bjørbæk, 2004; Sahu, 2003) and liver of obese human and mice (Brabant et al., 2005; Huang, Dedousis, Bhatt, & O'Doherty, 2004). Nonetheless, the same was not found in the kidney (Morgan, Thedens, Weiss, & Rahmouni, 2008; Rahmouni, Morgan, Morgan, Mark, & Haynes, 2005) and heart (Correia, Morgan, Sivitz, Mark, & Haynes, 2001; Mark, Correia, Rahmouni, & Haynes, 2002) of obese humans. We confirmed here, for the first time, the establishment of leptin resistance in the ovary of obese female mice. This represents an important finding concerning local action of leptin in follicular growth (Panwar et al., 2012), ovulation (Lisa Dupuis et al., 2014) and oocyte quality (Joo et al., 2010). Leptin action in the ovary is complex and its effects bimodal. Decreased leptin levels in the circulation were shown to facilitate the transition from primary to secondary follicles (Panwar et al., 2012),

but leptin was also shown to be required for ovulation, possibly supporting CC expansion through cyclooxygenase (COX) 2 and hyaluronic acid synthase (HAS) 2 activity (Lisa Dupuis et al., 2014). Indeed, Ryan and co-workers showed that leptin supported oocyte maturation from the germinal vesicle stage (Ryan et al., 2002). To our understanding, leptin in the ovary seems to be required at minimum levels in early stages of follicular development, whereas it appears to play a major role during ovulation and oocyte maturation (Duggal et al., 2000; Swain, Dunn, McConnell, Gonzalez-Martinez, & Smith, 2004). This assumption was corroborated also by the finding that *ob/ob* mice contain antral follicles in their ovaries (data not shown). Thus, altered leptin signalling during obesity could affect ovarian performance and fertility differently in both early and late obesity states.

Our first aim was to elucidate the molecular mechanisms leading to the establishment of leptin resistance in the obese ovary. The analysis of different ObRb Tyr domains highlighted a decrease in pTyr985 alongside pJAK2 in ovaries from 16wk HFD mice, concomitant with increased SOCS3 protein and decreased pSTAT5. It is well known that STAT3 promotes transcription of SOCS3, a key mediator of leptin resistance (Banks et al., 2000; Ernst et al., 2009), which can further block Tyr985 and Tyr1077 (Eyckerman, Broekaert, Verhee, Vandekerckhove, & Tavernier, 2000) to attenuate JAK2 phosphorylation (Babon et al., 2012). Functionally, STAT5 phosphorylation in the mouse ovary was shown to be key for prolactin signalling and cell proliferation during follicular growth (Bouilly, Sonigo, Auffret, & Gibori, 2012), as well as corpus luteum formation (Anderson, Isa, Barclay, Waters, & Curlewis, 2009) (Erlebacher, Zhang, Parlow, & Glimcher, 2004). Hence, reduced pSTAT5 signalling *per se* could jeopardise oocyte maturation and fertility during obesity. Importantly, we observed that SOCS3 staining in the oocyte originated mainly from ObRb activation, since the *ob/ob* mouse presented much weaker staining. This is suggestive of a direct impact of ovarian leptin signalling disruption on the oocyte. Indeed, at 16wk DIO, we observed different levels of *Socs3* transcribed in various ovarian components. Our RNAseq data revealed that *Socs3* was

increased at 4wk HFD, but decreased at 16wk HFD in CCs, whereas in the stroma/TC compartment it was upregulated in late obesity. This may indicate blunted ObRb signalling in CCs at 16wks HFD, once the transcription of major components of the pathway was inhibited (Figure 6 – figure supplement 1A). Therefore, leptin signalling in CCs seems to be very sensitive to obesity. This presents major implications for the oocyte, once the gamete is unable to use glucose and entirely depends on the metabolic performance of CCs for maturation (Sugiura, Pendola, & Eppig, 2005).

Having an understanding of the impact of obesity on leptin signalling in ovarian compartments, we then analysed the transcriptome of CCs isolated from LEPT, 4wk and 16wk DIO models. The use of the pharmacologically hyperleptinemic model allowed us to dissect the contribution of overactivation of ObRb in the major changes taking place in CCs during obesity. In 4 wk HFD, through activation of the JAK-STAT cascade, increased leptin seemed mainly to impair cellular trafficking and paracrine transfer of macromolecules. This is known to be a crucial process for the metabolic cooperation between the oocyte and somatic cells (Russell, Gilchrist, Brown, & Thompson, 2016b). Indeed, the genes *Micall1* and *Unc-51 Like Kinase (Ulk) 4* are important mediators of endocytosis (Giridharan, Cai, Vitale, Naslavsky, & Caplan, 2013; Pelkmans et al., 2005), and were shown to be regulated by *Stat3* in our network analysis. Another striking result was the coordinate downregulation of genes involved in cytoskeleton and actin-filament organisation in LEPT and 4 wk HFD (Figure 6C). As in axons, microtubules form the cytoskeletal core of granulosa cell transzonal projections (TZPs), that provide tracks for the polarized translocation of secretory pathway organelles (Albertini, Combelles, Benecchi, & Carabatsos, 2001). Thus, by impairing the intrinsic stability of TZPs in granulosa cells, leptin could be affecting the paracrine exchanges between oocytes and somatic cells, an instrumental system for oocyte maturation (Li & Albertini, 2013). Indeed, the oocyte is in extreme need of the metabolites generated in CCs, but also signalling factors such as growth differentiation factor (GDF) 9 secreted by the oocyte and required to orchestrate the

performance of CCs. Leptin seemed to support the TCA cycle at 4 wk HFD (Figure 6- figure supplement 1B), which suggests us that at this early obesity stage the boost in leptin signalling in CCs could be beneficial, following the positive response on oocyte competence and GDF9 signalling (Figure 6- figure supplement 1D). However, at 16 wk HFD the inferred drop in CC metabolic fitness was paralleled by a decrease in the main paracrine mediators of oocyte maturation and responsiveness to GDF9 (Figure 6- figure supplement 1B-D), which invariably compromises oocyte quality.

The aforementioned events described are an important part of COC expansion, a complex mechanism triggered by luteinizing hormone (LH), in which bidirectional exchange of metabolites and signaling factors between the oocyte and CCs leads to maturation of the gamete and resumption of meiosis (Dumesic, Meldrum, Katz-Jaffe, Krisher, & Schoolcraft, 2015). This process is tightly regulated by immune mediators, particularly IL6 (Liu et al., 2009). Also, the role of leptin in mediating inflammatory response (Fernández-Riejos et al., 2010), particularly innate immunity through IL6 has been described before. Consequently, the detrimental effect of obesity can be related to increased leptin signaling at 4 wk HFD, but most certainly through its failure at 16 wk HFD (Figure 6- figure supplement 1A).

In the final study we characterised the timing of the changes in gene signature in CCs throughout obesity. It was reassuring to see amongst the DEGs in both 4 wk and 16 wk DIO the processes initially impaired through downregulation of gene expression were cell membrane trafficking and ECM organisation, corroborating our previous findings. Then other genes presented a bimodal behaviour, such as *Atf7ip*, which was increased at 4 wk HFD and decreased at 16 wk HFD. The protein encoded by this gene is known to partner with SET Domain Bifurcated Histone Lysine Methyltransferase (SETDB) 1, and mediate methylation of lysine 9 of histone H3 (H3K9me), a hallmark of repressed heterochromatin (Becker, Nicetto, & Zaret, 2016). As previously characterised, together with TASOR, M-Phase Phosphoprotein (MPP) 8, and Periphilin, they form the HUSH complex, which deposits H3K9me3 and

mediates transcriptional repression at heterochromatic loci (Tchasovnikarova et al., 2015). Importantly, the level of the gene *Tasor* was significantly downregulated in LEPT and 4 wk HFD, suggestive of changes in H3K9me3 distribution in these cells, which deserves further attention. Furthermore, in LEPT and 4 wk HFD, there were additional epigenetic modifiers amongst DEGs, *Dnmt3a*, further evidence for the potential for epigenetic changes in these cells during obesity. Finally, amongst the three genes inhibited at 4 wk HFD but activated at 16 wk HFD, we found *Rhou*, a gene that regulates cell morphology (Tao et al., 2001). Considering also the high expression level of inflammatory mediators at this stage, the activated pathways may well be an outcome of lipotoxicity previously described in the obese ovary (Linda Lin-Yan Wu et al., 2010). Thus, during obesity ovarian cells are trying to accommodate the surplus of lipid compounds, which is likely to activate mechanisms of cellular reorganisation. Overall, early changes in CC transport, gene expression and epigenetic regulation are followed by mounting inflammatory pathways and cellular rearrangement to accommodate the lipid surplus.

In conclusion, we show that in the obese ovary inhibition of ObRb is mediated by SOCS3, which blocks pTyr985, pJAK2 and pSTAT5. Furthermore, we detected SOCS3 in the oocyte, highlighting the potential importance of local leptin signalling for oocyte quality. We also revealed that an obesogenic environment does not affect various ovarian compartments uniformly: CCs responded differently than the TC/stroma compartment to leptin signalling and thus could develop leptin resistance more rapidly. Of particular note, we showed that global transcriptome of CCs correlated globally with the BW. Finally, RNA-seq analysis of CCs showed not only major changes in gene signatures in early (4 wk HFD) and late (16 wk HFD) obesity, but also how leptin is contributing to those changes. At 4 wk HFD, leptin supported the upregulation of pathways like glucose metabolism, but was also inhibiting key functions such as gene expression and epigenetic regulation, as well as cytoskeleton organisation. Conversely, at 16 wk HFD CCs showed that gene signatures for the inflammatory response and cell morphogenesis were increased, and metabolism and transport decreased. Further studies

are being made to directly assess the genetic and epigenetic consequence of such changes in the oocyte.

MATERIALS AND METHODS

Animal protocol

Breeding pairs from the strains C57BL/6J (B6) and B6.Cg-Lep^{ob}/J (ob/ob) mice were obtained from the Jacksons Laboratory (The Jacksons Laboratory, Bar Harbor, Maine, USA). At 8 weeks of age B6 animals were divided into 2 groups (n=10/group). In DIO, control group was fed *ad libitum* chow diet (11% energy in kcal from fat, 5053, rodent diet 20, LabDiet IPS, London, UK), while experimental group received high fat diet (58% energy in kcal from fat, AIN-76A 9G03, LabDiet IPS). Mice were maintained under the diet for 4 or 16 wk. Regarding the pharmacological hyperleptinemia protocol, 8 wk old B6 female mice were divided into 4 groups (n=15/group): i) saline 9 d; ii) leptin 9 d; iii) saline 16 d; and iv) leptin 16 d (Recombinant Mouse Leptin, GFM26, Cell Guidance Systems, Cambridge, UK). The animals were injected intraperitoneally twice a day, at 09:00h and 21:00h and total dosage of 100 μg/day of leptin was administrated. Concerning *ob/ob* model, mice were kept from weaning until twelve wk of age on CD. For all protocols, mice were housed with a 12h light/12h dark cycle at room temperature. All experiments were approved by Local Committee for the Ethical Treatment of Experimental Animals of Warmia- Mazury University (Agreement No. 80/2015, 15/2018, 38/2018), Olsztyn, Poland.

For the phenotype characterisation of LEPT model, body composition changes were monitored every three days, while for DIO model every 4 weeks, by nuclear magnetic resonance (NMR, Bruker, Rheinstetten, Germany). Body weight, fat mass, lean mass (LM) and adiposity index (AI, fat mass/lean mass) were defined. Food intake was measured on a daily basis. For LEPT and DIO models vaginal cytology was assessed between 9:00h and 10:00h for six consecutive days. The results were analysed for percent of time spend in each estrous cycle

phase (Figure 1- figure supplement 1H, 1I; Figure 2- figure supplement 1F). After the vaginal saline lavage, the smears were placed on clean glass slides and stained with Diff Quik Staining Set (Diff- Quik Color Kit, Rapid Staining Set, Medion Grifols Diagnostics AG, Duedingen, Switzerland) in order to identify cells present in smears. The results were analysed as follows: at diestrous only leukocytes accompanied by few epithelial nucleated cells could be observed, at proestrous mostly nucleated and few cornified cells were present along with some leukocytes, at estrous only cornified cells were present, while at metestrous cornified epithelial cells and leukocytes were identified.

Superovulation protocol was used for *cumulus oophorous complex* collection and further pure cumulus cells isolation after removing the metaphase II (MII) oocytes. The animals were injected with pregnant mare's serum gonadotropin (PMSG, G4877, 5IU, Sigma Aldrich, Saint Louis, Missouri, USA) followed after 48-h interval by human chorionic gonadotropin (hCG, Chorulon, 5IU, MSD Animal Health, Boxmeer, Holland). 18-hr after hCG injection, animals were sacrificed.

Ovary collections

Mice were sacrificed by cervical dislocation and reproductive tracts were collected and rinsed with phosphate buffered saline (PBS, 0.1M, pH=7.4). Ovaries were removed from the genitalia and the adipose tissue was cleaned off. Ovaries were stored either in TRI Reagent (T9424, Sigma Aldrich) for mRNA, or radioimmunoprecipitation assay buffer (RIPA, 89901, ThermoFisher Scientific, Waltham, Massachusetts, USA) and protease inhibitors, after adding protease inhibitor cocktail (PIC, P8340, Sigma Aldrich), phenylmethanesulfonyl fluoride (PMSF, P7626, Sigma Aldrich) and phosphatase inhibitor (88667, Thermo Fisher Scientific) for protein analysis. Samples were stored in -80°C, except for phosphorylated protein which were isolated immediately after sacrificing the animals.

Ovarian cell isolation protocol

Immediately after collections, ovaries were transferred to Dulbecco's modified Eagle's medium (DMEM, D/F medium; 1:1 [v/v], D-8900, Sigma Aldrich) with 3% bovine serum albumin (BSA, 735078, Roche Diagnostics GmbH, Mannheim, Germany), 20 µg/ml gentamicin (G1397, Sigma Aldrich) and 250 µg/ml amphotericin (A2942, Sigma Aldrich). For theca/stroma cell isolation, ovaries were punctured with a 16 gauge needle as described before (Couse et al., 2006). Briefly, after removing all follicles and oocytes the remaining tissue was washed twice with media and stored in TRI Reagent for mRNA analysis.

RNA isolation and cDNA synthesis

For mRNA extraction, either whole ovaries, or enriched theca/stroma fraction were mechanically disrupted with a lancet in 1ml of TRI Reagent in 1,5ml eppendorf tubes (n=8/group). The suspension was pipetted up and down vigorously and incubated for 5min in room temperature (RT). After centrifugation of the samples at 9400g and 4°C for 15min, the supernatant was transferred to a new tube and thoroughly mixed with 100µl of 1-Bromo-3-chloropropan (BCP, BP151, Molecular Research Centre, Cincinnati, Ohio, USA), followed by a RT incubation of 10 min. Further on, samples were centrifuged (15min, 13500g, 4°C) and the aqueous phase was transferred to a new tube. In the next step, the samples were mixed with equal volume of isopropanol and incubated in -80°C for 60 min followed by a centrifugation at 20000g, 4°C, for 15min to pellet down the mRNA, which was then washed three times with 75% ethanol and incubated overnight in -80°C. The next day, samples were centrifuged (15min, 20000g, 4°C) and mRNA pellet was dried out and resuspended in 20µl of RNAse free water (W4502, Sigma Aldrich) with RNAse Inhibitor (RiboProtect, RT35, BLIRT, Gdańsk, Poland). Then, the mRNA quality and concentration were confirmed on NanoDrop machine. The ratio of absorbance at 260nm and 280 nm (A260/A280) was defined to check the quality and quantity of isolated mRNA. A total of 1 µg of mRNA was reversely transcribed using Maxima

First Strand cDNA Synthesis Kit for Real time polymerase chain reaction (RT-qPCR) (K1642, ThermoScientific) according to the manufacturer's instructions. The cDNA was stored in -20°C until the real-time PCR was carried out.

Real time polymerase chain reaction

Real-time PCR assay was performed in a 7900 Real Time PCR System (Applied Biosystems, Warrington, UK) using Maxima SYBR Green/ROX qPCR Master Mix (K0223, ThermoScientific). The primers were designed using Primer 3.0 v.0.4.0. software (Koressaar & Remm, 2007; Untergasser et al., 2012), based on gene sequences in GeneBank (NCBI) as described before (Galvão, Wolodko, Rebordão, Skarzynski, & Ferreira-Dias, 2018). All primers were synthesized by Sigma Aldrich. Primer sequences, expected PCR products length, and GeneBank accession numbers are reported in Supplementary file 1 Table 1. The total reaction volume was 12 μL, containing 4μL cDNA (10µg), 1μL each forward and reverse primers (80nM or 160nM), and 6 μL SYBR Green PCR master mix. Real-time PCR was carried out as follows: initial denaturation (10 min at 95°C), followed by 45 cycles of denaturation (15s at 95°C) and annealing (1 min at 60°C). After each PCR reaction, melting curves were obtained by stepwise increases in temperature from 60 to 95°C to ensure single product amplification. In each real-time assay, both the target gene and a housekeeping gene (HKG) *Ribosomal Protein L32* (*Rpl32*, primers Supplementary file 1 Table 1) or *Eukaryotic Translation Initiation Factor 5A* (*Eif5a*, primers Supplementary file 1 Table 1) were run simultaneously and reactions were carried out in duplicate wells on a 384 well optical reaction plate (4306737, Applied Biosystems). HKG was selected after NormFinder analysis of the most stable gene in each experimental group. Real time results were analysed with the Real-time PCR Miner algorithm (Zhao & Fernald, 2005).

Western blotting

Protein expression was assessed by western blotting (n=5/group). Ovaries in RIPA with protease and phosphatase inhibitors were mechanically disrupted with a lancet. Then, lysates were incubated for one hour on ice with mixing every 15 mins. Subsequently, samples were centrifuged at 20000g for 15min, 4°C, and the supernatant was collected and stored in -80°C until the analysis. The protein concentration was assessed using bicinchoninic acid assay (BCA, BCA1-1KT, Sigma Aldrich). A total of 10-40μg of protein was loaded on 8-14% acrylamide gel, and after electrophoresis proteins were transferred to the polyvinylidene difluoride (PVDF) or nitrocellulose membrane regarding the antibodies. The membranes were blocked in 5% BSA (A2153, Sigma Aldrich) and incubated with primary antibodies (AB) overnight at 4°C. Leptin receptor and its phosphorylated domains were evaluated using the following antibodies: mouse monoclonal (MM) against leptin receptor (ObR; 1:500, cat# sc-8391, Santa Cruz Biotechnology, Dallas, Texas, USA), goat polyclonal (GP) against phosphorylated Tyr 985 ObRb (pTyr985ObRb; 1:500, cat# sc-16419, Santa Cruz Biotechnology), rabbit polyclonal (RP) against phosphorylated Tyr 1077 ObRb (pTyr1077ObR; 1:500, cat# 07-1317, Merck Millipore, Burlington, Vermont, USA), GP against phosphorylated Tyr 1138 ObRb (pTyr1138ObRb; 1:500, cat# sc-16421, Santa Cruz Biotechnology). The expression of leptin signalling pathway components was assessed using the following antibodies- RP against Jak2 (1:200, cat# sc-294, Santa Cruz Biotechnology), RP against phosphorylated Tyr 1007/1008 Jak2 (pJak2; 1:200, cat# sc-16566-R, Santa Cruz Biotechnology), RP against STAT3 (1:200, cat# sc-482, Santa Cruz Biotechnology), MM against phosphorylated Tyr 705 pSTAT3 (1:200, cat# sc-8059, Santa Cruz Biotechnology), GP against PTP1B (1:200, cat# sc-1718, Santa Cruz Biotechnology), MM against SOCS3 (1:500, cat# sc-51699, Santa Cruz Biotechnology) in cell lysates. The results were normalized to β-actin level (β-actin, 1:10000, MM, cat# A2228, Sigma-Aldrich). All antibodies specifications are summarised in Supplementary file 2 Table 2.

Then, proteins were detected by incubating the membrane with a secondary GP against rabbit alkaline phosphatase-conjugated (1:30000, cat# A3687, Sigma Aldrich), GP against mouse alkaline phosphatase-conjugated (1:20000, cat# 31321, ThermoScientific), RP against goat alkaline phosphatase-conjugated (1:30000, cat# A4187, Sigma Aldrich) antibodies, RP against goat horseradish peroxidase- conjugated (1:75000, cat# A50-100P, Bethyl, Montgomery, Alabama, USA) for 2h at RT. Immune complexes were visualized using the alkaline phosphatase visualization procedure or ECL substrate visualization. Blots were scanned in Molecular Imager VersaDoc MP 4000 System (BioRad, Hercules, California, USA) and specific bands quantified using ImageLab Software (BioRad). At last, band density for each of the target protein was normalized against β-actin.

Immunohistochemistry and Immunofluorescent stainings

Ovaries were fixed in 4% neutral phosphate-buffered formalin (NBF, 432173427, Poch, Gliwice, Poland) at 4°C for 24h and subsequently dehydrated in ethanol. The paraffin embedded ovarian tissue samples were sectioned into 5μm slices. For antigen retrieval, sections were heated in citrate buffer (10mM, pH=6,0). Tissue was blocked with blocking solution (ab64261, Abcam, Cambridge, UK) for 1h at RT and incubated with RP against SOCS3 antibody (1:1000, ab16030, Abcam) and PTP1B antibody (1:500, ab189179, Abcam) overnight at 4°C. The negative control sections were incubated with RP against immunoglobulin G (IgG, cat# ab37415, Abcam) or without primary antibody. The primary antibody complexes were detected after incubating the tissue with biotinylated goat anti-rabbit IgG (H+L) (ab64261, Abcam) for 60 min, and streptavidin peroxidase for 40min. Staining was evident after 15s incubation in 3,3-diaminobenzidine (DAB) peroxidase substrate solution (Rabbit-specific HRP/DAB (ABC) Detection IHC Kit, ab64261, Abcam). Subsequently, before samples were mounted, the counterstaining with haematoxylin (MHS16, Sigma Aldrich) was performed. Sections were examined using Axio Observer Systems Z1 microscope (Carl Zeiss

Microscopy GmbH, Hannover, Germany) and Zeiss ZEN 2.5 lite Microscope Software (Carl Zeiss, Germany). For immunofluorescent stainings, the 5μm cuts were deparaffinise and rehydrated in serious of alcohols. Then the tissues were permeabilized in 0,3% Triton X-100 (T8787, Sigma Aldrich), followed by antigen retrieval in citrate buffer (10mM, pH=6,0) for 40 min in 90°C and blocking in 2% BSA (A2153, Sigma Aldrich) with 0,3M glycine (G8898, Sigma Aldrich) in PBS-0,1% Tween 20 (P7949, Sigma Aldrich) (PBST) solution. Then the sections were incubated with 0,3% Sudan Black (199664, Sigma Aldrich) in 70% ethanol for 10 min in RT followed by washes in PBST. After that the slides were incubated with RP against SOCS3 antibody (1:200, ab16030, Abcam) overnight at 4°C. The negative control sections were incubated with RP against immunoglobulin G (IgG, cat# ab37415, Abcam) or without primary antibody. The next day slides were washed in PBST, followed by incubation with Cy3- donkey polyclonal anti-rabbit IgG (H+L) (711-165-152, Jackson ImmunoReserach, Cambridgeshire, UK), and series of washes in PBST. Finally, the slides were covered with drop of Prolong Gold medium with DAPI and closed with cover glass. The images were captured using an immerse objectives 40x/1.2A, 63x/1.4A on LSM800 confocal microscope (Carl Zeiss, Germany).

Enzyme- linked immunosorbent assay

After sacrificing the animals, blood was collected by heart puncturing and centrifuged immediately (180g, 10min, 4°C). Plasma was collected and stored in -80°C until the analysis was performed. Level of circulating adiponectin, leptin and insulin was assessed in ELISA test according to the manufacturer's instructions (Mouse Adiponectin ELISA Kit, EZMADP-60K, Merck Millipore; Mouse Leptin ELISA Kit, 90030; Crystal Chem, Zaandam, Netherlands; Rat/Mouse Insulin ELISA Kit, cat no EZRMI-13K; Merck Millipore). The intra- and interassay coefficients of variation (CVs) were as follows: for Adiponectin ELISA kit 5,4% and 1,4%, for Leptin ELISA kit <10% both and for Insulin ELISA kit 8,35% and 17.9%, respectively.

In order to determine the level of SOCS3 in ovarian extract, ELISA test was performed (ELISA KIT for SOCS3; cat no SEB684Mu, Cloud- Clone, Katy, Texas, USA). Briefly, the tissue was minced in lysis buffer, centrifuged (10000g, 5min, 4°C) and the protein concentration in the lysate was determined in BCA test. After performing ELISA test, the SOCS3 concentration was normalised for the equal amount of protein.

Cumulus cells collection and RNAseq library generation

A total of approximately 50 CC were collected from one individual COCs after digesting with hyaluronidase (H3506, 400 μg/ml, Sigma Aldrich) and removing the oocytes,, pure cumulus cells were obtained after superovulation of female mice from either 4 wk and 16 wk DIO (n=5/condition) or 16 d LEPT (n=3/condition) protocols. CCs were collected into RLT buffer (1053393, Qiagen, Hilden, Germany) and kept in -80°C until library generation. Subsequently, RNAseq libraries were prepared following the protocol previously validated (Picelli et al., 2013, 2014), with minor changes. Briefly, the mRNA was captured using Smart-seq2 oligo-dT pre-annealed to magnetic beads (MyOne C1, Invitrogen, Carlsbad, California, USA). The beads were resuspended in 10 μl of reverse transcriptase mix (100 U, SuperScript II, Invitrogen; 10 U, RNAsin, Promega, Madison, Wisconsin, USA), 1 × Superscript II First-Strand Buffer, 2.5 mM ditiotreitol (DTT, Invitrogen), 1 M betaine (Sigma Aldrich), 9 mM magnesium chloride ($MgCl_2$, Invitrogen), 1 μM Template-Switching Oligo (Exiqon, Vedbaek, Denmark), 1 mM deoxyribonucleotide triphosphate (dNTP) mix (Roche) and incubated for 60 min at 42 °C followed by 30 min at 50 °C and 10 min at 60 °C (Picelli et al., 2013, 2014). Amplification of the cDNA was then undertaken after adding 11 μl of 2 × KAPA HiFi HotStart ReadyMix and 1 μl of 2 μM ISPCR primer (Picelli et al., 2013, 2014), followed by the cycle: 98°C for 3 min, then 9 cycles of 98°C for 15 s, 67°C for 20 s, 72°C for 6 min and finally 72°C for 5 min. Finally, the cDNA was purified using similar volume of AMPure beads (Beckman Coulter, Brea, California, USA) and eluted into 20 μl of water. All

libraries were prepared from 100 to 200 pg of cDNA using the Nextera XT Kit (Illumina, San Diego, California, USA), regarding the manufacturer's instructions. The final cDNA library was purified using a 0.7:1 volumetric ratio of AMPure beads before pooling and sequencing with 75-base pair (bp) single-read high output Illumina Nextseq500. A total of 5-10 million mappable reads per sample were obtained, with an average of 30-50 million reads per condition.

Library mapping and trimming

Trim galore v0.4.2 was used with default parameters on raw fastq sequence files. Mapping of the RNAseq data was done with Hisat v2.0.5 against the mouse GRCm38 genome, as guided by known splice sites taken from Ensemble v68.

RNAseq differential expression analysis

Mapped RNAseq reads were quantified and analysed using SeqMonk version v1.45.4 (http://www.bioinformatics.babraham.ac.uk/projects/seqmonk/). Differential expression analysis was performed using DESeq2 (Love, Huber, & Anders, 2014) implemented in Seqmonk setting an FDR < 0.05.

Gene co-expression network analysis

DESeq2 normalised counts were used to estimate pairwise correlations and define the edges of the network (r > 0.90). Glay community clustering (G. Su, Kuchinsky, Morris, States, & Meng, 2010) was implemented in Cytoscape version 3.4.0 (Shannon et al., 2003) to partition the network into clusters. Biological function enrichment of the network was performed using ClueGo (Bindea et al., 2009).

Statistical analysis

Statistical analysis was performed using GraphPad Prism 7.0. The D'Agostino-Pearson omnibus normality test was performed. Nonparametric Mann-Whitney test or multiple unpaired t-test with statistical significance determined using the Bonferroni- Sidak method, depending on the experiment. The data are shown as the mean ± SD of three or more independent replicates. Significance was defined as values of $p < 0.05$.

AKNOWLEDGEMENTS

Work supported by Polish NCN GRANTs - National Centre for Science (No. 2014/15/D/NZ4/01152 and 2016/23/B/NZ4/03737); A. G. was supported by Horizon 2020 Marie Curie Individual Fellowship. Work in GK's group is supported by grants from the UK Biotechnology and Biological Sciences Research Council and Medical Research Council (BBS/E/B/000C0423, MR/K011332/1, MR/S000437/1). We would like to thank Dr Jorg Morf for the constructive discussion and suggestions on the analysis of the transcriptome data; Dr Daniel Murta for providing the of mouse ovaries cuts; and Dr Fatima Santos and Krzysztof Witek for providing technical support with the imaging and confocal microscopy.

REFERENCES

Abou-Zeid, N., Pandjaitan, R., Sengmanivong, L., David, V., Le Pavec, G., Salamero, J., & Zahraoui, A. (2011). MICAL-like1 mediates epidermal growth factor receptor endocytosis. *Molecular Biology of the Cell*, *22*(18), 3431–3441. https://doi.org/10.1091/mbc.E11-01-0030

Adriaenssens, T., Mazoyer, C., Segers, I., Wathlet, S., & Smitz, J. (2009). Differences in Collagen Expression in Cumulus Cells after Exposure to Highly Purified Menotropin or Recombinant Follicle-Stimulating Hormone in a Mouse Follicle Culture Model1. *Biology of Reproduction*, *80*(5), 1015–1025. https://doi.org/10.1095/biolreprod.107.067462

AHREN, B. (1999). Plasma leptin and insulin in C57Bl/6J mice on a high-fat diet: relation to subsequent changes in body weight. *Acta Physiologica Scandinavica*, *165*(2), 233–240. https://doi.org/10.1046/j.1365-201x.1999.00518.x

Al Maskari, M. Y., & Alnaqdy, A. A. (2006). Correlation between Serum Leptin Levels, Body Mass Index and Obesity in Omanis. *Sultan Qaboos University Medical Journal*, *6*(2), 27–

31. Retrieved from http://www.ncbi.nlm.nih.gov/pubmed/21748132

Albertini, D. F., Combelles, C. M., Benecchi, E., & Carabatsos, M. J. (2001). Cellular basis for paracrine regulation of ovarian follicle development. *Reproduction (Cambridge, England)*, *121*(5), 647–653. Retrieved from http://www.ncbi.nlm.nih.gov/pubmed/11427152

Anderson, S. T., Isa, N. N. M., Barclay, J. L., Waters, M. J., & Curlewis, J. D. (2009). Maximal expression of suppressors of cytokine signaling in the rat ovary occurs in late pregnancy. *REPRODUCTION*, *138*(3), 537–544. https://doi.org/10.1530/REP-08-0425

Babon, J. J., Kershaw, N. J., Murphy, J. M., Varghese, L. N., Laktyushin, A., Young, S. N., … Nicola, N. A. (2012). Suppression of cytokine signaling by SOCS3: characterization of the mode of inhibition and the basis of its specificity. *Immunity*, *36*(2), 239–250. https://doi.org/10.1016/j.immuni.2011.12.015

Banks, A. S., Davis, S. M., Bates, S. H., & Myers, M. G. (2000). Activation of downstream signals by the long form of the leptin receptor. *The Journal of Biological Chemistry*, *275*(19), 14563–14572. https://doi.org/10.1074/JBC.275.19.14563

Becker, J. S., Nicetto, D., & Zaret, K. S. (2016). H3K9me3-Dependent Heterochromatin: Barrier to Cell Fate Changes. *Trends in Genetics*, *32*(1), 29–41. https://doi.org/10.1016/j.tig.2015.11.001

Bindea, G., Mlecnik, B., Hackl, H., Charoentong, P., Tosolini, M., Kirilovsky, A., … Galon, J. (2009). ClueGO: a Cytoscape plug-in to decipher functionally grouped gene ontology and pathway annotation networks. *Bioinformatics*, *25*(8), 1091. https://doi.org/10.1093/BIOINFORMATICS/BTP101

Bjørbaek, C., & Kahn, B. B. (2004). Leptin signaling in the central nervous system and the periphery. *Recent Progress in Hormone Research*, *59*, 305–331. Retrieved from http://www.ncbi.nlm.nih.gov/pubmed/14749508

Bjørbæk, C., Lavery, H. J., Bates, S. H., Olson, R. K., Davis, S. M., Flier, J. S., & Myers, M. G. (2000). SOCS3 Mediates Feedback Inhibition of the Leptin Receptor via Tyr ^{985}. *Journal of Biological Chemistry*, *275*(51), 40649–40657. https://doi.org/10.1074/jbc.M007577200

Bouilly, J., Sonigo, C., Auffret, J., & Gibori, G. (2012). Prolactin signaling mechanisms in ovary. *Molecular and Cellular Endocrinology*, *356*(1–2), 80–87. https://doi.org/10.1016/J.MCE.2011.05.004

Brabant, G., Müller, G., Horn, R., Anderwald, C., Roden, M., & Nave, H. (2005). Hepatic leptin signaling in obesity. *FASEB Journal□: Official Publication of the Federation of American Societies for Experimental Biology*, *19*(8), 1048–1050. https://doi.org/10.1096/fj.04-2846fje

Cava, A. La, & Matarese, G. (2004). The weight of leptin in immunity. *Nature Reviews Immunology*, *4*(5), 371–379. https://doi.org/10.1038/nri1350

Cetica, P., Pintos, L., Dalvit, G., & Beconi, M. (2002). Activity of key enzymes involved in glucose and triglyceride catabolism during bovine oocyte maturation in vitro. *Reproduction (Cambridge, England)*, *124*(5), 675–681. Retrieved from http://www.ncbi.nlm.nih.gov/pubmed/12417006

Correia, M. L., Morgan, D. A., Sivitz, W. I., Mark, A. L., & Haynes, W. G. (2001). Leptin acts in the central nervous system to produce dose-dependent changes in arterial pressure. *Hypertension (Dallas, Tex.□: 1979)*, *37*(3), 936–942. Retrieved from http://www.ncbi.nlm.nih.gov/pubmed/11244021

Couse, J. F., Yates, M. M., Rodriguez, K. F., Johnson, J. A., Poirier, D., & Korach, K. S. (2006). The Intraovarian Actions of Estrogen Receptor-α Are Necessary to Repress the Formation of Morphological and Functional Leydig-Like Cells in the Female Gonad. *Endocrinology*, *147*(8), 3666–3678. https://doi.org/10.1210/en.2006-0276

Dağ, Z. Ö., & Dilbaz, B. (2015). Impact of obesity on infertility in women. *Journal of the Turkish German Gynecological Association*, *16*(2), 111–117. https://doi.org/10.5152/jtgga.2015.15232

Duan, J., Choi, Y.-H., Hartzell, D., Della-Fera, M. A., Hamrick, M., & Baile, C. A. (2007). *Effects of Subcutaneous Leptin Injections on Hypo-thalamic Gene Profiles in Lean and ob/ob Mice*. https://doi.org/10.1038/oby.2007.314

Duggal, P. S., Van der Hoek, K. H., Milner, C. R., Ryan, N. K., Armstrong, D. T., Magoffin, D. A., & Norman, R. J. (2000). The *in Vivo* and *in Vitro* Effects of Exogenous Leptin on Ovulation in the Rat [1]. *Endocrinology*, *141*(6), 1971–1976. https://doi.org/10.1210/endo.141.6.7509

Dumesic, D. A., Meldrum, D. R., Katz-Jaffe, M. G., Krisher, R. L., & Schoolcraft, W. B. (2015). Oocyte environment: follicular fluid and cumulus cells are critical for oocyte health. *Fertility and Sterility*, *103*(2), 303–316. https://doi.org/10.1016/j.fertnstert.2014.11.015

Dunning, K. R., Watson, L. N., Zhang, V. J., Brown, H. M., Kaczmarek, A. K., Robker, R. L., & Russell, D. L. (2015). Activation of Mouse Cumulus-Oocyte Complex Maturation In Vitro Through EGF-Like Activity of Versican1. *Biology of Reproduction*, *92*(5), 116. https://doi.org/10.1095/biolreprod.114.127274

Dupuis, L., Schuermann, Y., Cohen, T., Siddappa, D., Kalaiselvanraja, A., Pansera, M., … Duggavathi, R. (2013). Role of leptin receptors in granulosa cells during ovulation. *Reproduction*, *147*(2), 221–229. https://doi.org/10.1530/REP-13-0356

Dupuis, Lisa, Schuermann, Y., Cohen, T., Siddappa, D., Kalaiselvanraja, A., Pansera, M., … Duggavathi, R. (2014). Role of leptin receptors in granulosa cells during ovulation. *Reproduction*, *147*(2), 221–229. https://doi.org/10.1530/REP-13-0356

Eden, E., Lipson, D., Yogev, S., & Yakhini, Z. (2007). Discovering Motifs in Ranked Lists of DNA Sequences. *PLoS Computational Biology*, *3*(3), e39. https://doi.org/10.1371/journal.pcbi.0030039

Eden, E., Navon, R., Steinfeld, I., Lipson, D., & Yakhini, Z. (2009). GOrilla: a tool for discovery and visualization of enriched GO terms in ranked gene lists. *BMC Bioinformatics*, *10*(1), 48. https://doi.org/10.1186/1471-2105-10-48

Englert, N. A., Luo, G., Goldstein, J. A., & Surapureddi, S. (2015). Epigenetic modification of histone 3 lysine 27: mediator subunit MED25 is required for the dissociation of polycomb repressive complex 2 from the promoter of cytochrome P450 2C9. *The Journal of Biological Chemistry*, *290*(4), 2264–2278. https://doi.org/10.1074/jbc.M114.579474

Erlebacher, A., Zhang, D., Parlow, A. F., & Glimcher, L. H. (2004). Ovarian insufficiency and early pregnancy loss induced by activation of the innate immune system. *The Journal of Clinical Investigation*, *114*(1), 39–48. https://doi.org/10.1172/JCI20645

Ernst, M. B., Wunderlich, C. M., Hess, S., Paehler, M., Mesaros, A., Koralov, S. B., … Wunderlich, F. T. (2009). Enhanced Stat3 activation in POMC neurons provokes negative feedback inhibition of leptin and insulin signaling in obesity. *The Journal of Neuroscience : The Official Journal of the Society for Neuroscience*, *29*(37), 11582–11593. https://doi.org/10.1523/JNEUROSCI.5712-08.2009

Eyckerman, S., Broekaert, D., Verhee, A., Vandekerckhove, J., & Tavernier, J. (2000). Identification of the Y985 and Y1077 motifs as SOCS3 recruitment sites in the murine leptin receptor. *FEBS Letters*, *486*(1), 33–37. https://doi.org/10.1016/S0014-5793(00)02205-5

Faggioni, R., Fantuzzi, G., Fuller, J., Dinarello, C. A., Feingold, K. R., & Grunfeld, C. (1998). IL-1β mediates leptin induction during inflammation. *American Journal of Physiology-Regulatory, Integrative and Comparative Physiology*, *274*(1), R204–R208. https://doi.org/10.1152/ajpregu.1998.274.1.R204

Fantuzzi, G., & Faggioni, R. (2000). Leptin in the regulation of immunity, inflammation, and hematopoiesis. *Journal of Leukocyte Biology*, *68*(4), 437–446. Retrieved from http://www.ncbi.nlm.nih.gov/pubmed/11037963

Fernández-Riejos, P., Najib, S., Santos-Alvarez, J., Martín-Romero, C., Pérez-Pérez, A.,

González-Yanes, C., & Sánchez-Margalet, V. (2010). Role of Leptin in the Activation of Immune Cells. *Mediators of Inflammation*, *2010*, 1–8. https://doi.org/10.1155/2010/568343

Frank, L. A., Sutton-McDowall, M. L., Gilchrist, R. B., & Thompson, J. G. (2014). The effect of peri-conception hyperglycaemia and the involvement of the hexosamine biosynthesis pathway in mediating oocyte and embryo developmental competence. *Molecular Reproduction and Development*, *81*(5), 391–408. https://doi.org/10.1002/mrd.22299

Friedman, J. M., & Halaas, J. L. (1998). Leptin and the regulation of body weight in mammals. *Nature*, *395*(6704), 763–770. https://doi.org/10.1038/27376

Galvão, A., Wolodko, K., Rebordão, M. R., Skarzynski, D., & Ferreira-Dias, G. (2018). TGFB1 modulates in vitro secretory activity and viability of equine luteal cells. *Cytokine*, *110*, 316–327. https://doi.org/10.1016/J.CYTO.2018.03.038

Giridharan, S. S. P., Cai, B., Vitale, N., Naslavsky, N., & Caplan, S. (2013). Cooperation of MICAL-L1, syndapin2, and phosphatidic acid in tubular recycling endosome biogenesis. *Molecular Biology of the Cell*, *24*(11), 1776–1790. https://doi.org/10.1091/mbc.e13-01-0026

Gong, Y., Ishida-Takahashi, R., Villanueva, E. C., Fingar, D. C., Münzberg, H., & Myers, M. G. (2007). The Long Form of the Leptin Receptor Regulates STAT5 and Ribosomal Protein S6 via Alternate Mechanisms. *Journal of Biological Chemistry*, *282*(42), 31019–31027. https://doi.org/10.1074/jbc.M702838200

Haines, R. J., Pendleton, L. C., & Eichler, D. C. (2011). Argininosuccinate synthase: at the center of arginine metabolism. *International Journal of Biochemistry and Molecular Biology*, *2*(1), 8–23. Retrieved from http://www.ncbi.nlm.nih.gov/pubmed/21494411

Herrid, M., Nguyen, V. L., Hinch, G., & McFarlane, J. R. (2006). Leptin has concentration and stage-dependent effects on embryonic development in vitro. *Reproduction (Cambridge, England)*, *132*(2), 247–256. https://doi.org/10.1530/rep.1.01083

Huang, W., Dedousis, N., Bhatt, B. A., & O'Doherty, R. M. (2004). Impaired activation of phosphatidylinositol 3-kinase by leptin is a novel mechanism of hepatic leptin resistance in diet-induced obesity. *The Journal of Biological Chemistry*, *279*(21), 21695–21700. https://doi.org/10.1074/jbc.M401546200

Iikuni, N., Lam, Q. L. K., Lu, L., Matarese, G., & La Cava, A. (2008). Leptin and Inflammation. *Current Immunology Reviews*, *4*(2), 70–79. https://doi.org/10.2174/157339508784325046

Jimenez, P. T., Frolova, A. I., Chi, M. M., Grindler, N. M., Willcockson, A. R., Reynolds, K. A., … Moley, K. H. (2013). DHEA-Mediated Inhibition of the Pentose Phosphate Pathway Alters Oocyte Lipid Metabolism in Mice. *Endocrinology*, *154*(12), 4835–4844. https://doi.org/10.1210/en.2012-2140

Joo, J.-K., Joo, B.-S., Kim, S.-C., Choi, J.-R., Park, S.-H., & Lee, K.-S. (2010). Role of leptin in improvement of oocyte quality by regulation of ovarian angiogenesis. *Animal Reproduction Science*, *119*(3–4), 329–334. https://doi.org/10.1016/j.anireprosci.2010.02.002

Kloek, C., Haq, A. K., Dunn, S. L., Lavery, H. J., Banks, A. S., & Myers, M. G. (2002). Regulation of Jak kinases by intracellular leptin receptor sequences. *The Journal of Biological Chemistry*, *277*(44), 41547–41555. https://doi.org/10.1074/jbc.M205148200

Koressaar, T., & Remm, M. (2007). Enhancements and modifications of primer design program Primer3. *Bioinformatics*, *23*(10), 1289–1291. https://doi.org/10.1093/bioinformatics/btm091

Kuo, Y.-C., Shen, Y.-R., Chen, H.-I., Lin, Y.-H., Wang, Y.-Y., Chen, Y.-R., … Kuo, P.-L. (2015). SEPT12 orchestrates the formation of mammalian sperm annulus by organizing core octameric complexes with other SEPT proteins. *Journal of Cell Science*, *128*(5), 923–934. https://doi.org/10.1242/JCS.158998

Li, R., & Albertini, D. F. (2013). The road to maturation: somatic cell interaction and self-organization of the mammalian oocyte. *Nature Reviews Molecular Cell Biology*, *14*(3), 141–152. https://doi.org/10.1038/nrm3531

Liu, Z., de Matos, D. G., Fan, H.-Y., Shimada, M., Palmer, S., & Richards, J. S. (2009). Interleukin-6: An Autocrine Regulator of the Mouse Cumulus Cell-Oocyte Complex Expansion Process. *Endocrinology*, *150*(7), 3360–3368. https://doi.org/10.1210/en.2008-1532

Louis, G. W., Greenwald-Yarnell, M., Phillips, R., Coolen, L. M., Lehman, M. N., & Myers, M. G. (2011). Molecular Mapping of the Neural Pathways Linking Leptin to the Neuroendocrine Reproductive Axis. *Endocrinology*, *152*(6), 2302–2310. https://doi.org/10.1210/en.2011-0096

Love, M. I., Huber, W., & Anders, S. (2014). Moderated estimation of fold change and dispersion for RNA-seq data with DESeq2. *Genome Biology*, *15*(12), 550. https://doi.org/10.1186/s13059-014-0550-8

Maffei, M., Halaas, J., Ravussin, E., Pratley, R. E., Lee, G. H., Zhang, Y., … Friedman, J. M. (1995). Leptin levels in human and rodent: Measurement of plasma leptin and ob RNA in obese and weight-reduced subjects. *Nature Medicine*, *1*(11), 1155–1161. https://doi.org/10.1038/nm1195-1155

Mark, A. L., Correia, M. L. G., Rahmouni, K., & Haynes, W. G. (2002). Selective leptin resistance: a new concept in leptin physiology with cardiovascular implications. *Journal of Hypertension*, *20*(7), 1245–1250. Retrieved from http://www.ncbi.nlm.nih.gov/pubmed/12131511

Mirsaeidi, M., Gidfar, S., Vu, A., & Schraufnagel, D. (2016). Annexins family: insights into their functions and potential role in pathogenesis of sarcoidosis. *Journal of Translational Medicine*, *14*(1), 89. https://doi.org/10.1186/s12967-016-0843-7

Morgan, D. A., Thedens, D. R., Weiss, R., & Rahmouni, K. (2008). Mechanisms mediating renal sympathetic activation to leptin in obesity. *American Journal of Physiology-Regulatory, Integrative and Comparative Physiology*, *295*(6), R1730–R1736. https://doi.org/10.1152/ajpregu.90324.2008

Münzberg, H., Flier, J. S., & Bjørbæk, C. (2004). Region-Specific Leptin Resistance within the Hypothalamus of Diet-Induced Obese Mice. *Endocrinology*, *145*(11), 4880–4889. https://doi.org/10.1210/en.2004-0726

Mütze, J., Roth, J., Gerstberger, R., & Hübschle, T. (2007). Nuclear translocation of the transcription factor STAT5 in the rat brain after systemic leptin administration. *Neuroscience Letters*, *417*(3), 286–291. https://doi.org/10.1016/j.neulet.2007.02.074

Panwar, S., Herrid, M., Kauter, K. G., & McFarlane, J. R. (2012). Effect of passive immunization against leptin on ovarian follicular development in prepubertal mice. *Journal of Reproductive Immunology*, *96*(1–2), 19–24. https://doi.org/10.1016/J.JRI.2012.07.004

Pasquali, R., Patton, L., & Gambineri, A. (2007). Obesity and infertility. *Current Opinion in Endocrinology, Diabetes and Obesity*, *14*(6), 482–487. https://doi.org/10.1097/MED.0b013e3282f1d6cb

Pelkmans, L., Fava, E., Grabner, H., Hannus, M., Habermann, B., Krausz, E., & Zerial, M. (2005). Genome-wide analysis of human kinases in clathrin- and caveolae/raft-mediated endocytosis. *Nature*, *436*(7047), 78–86. https://doi.org/10.1038/nature03571

Picelli, S., Björklund, Å. K., Faridani, O. R., Sagasser, S., Winberg, G., & Sandberg, R. (2013). Smart-seq2 for sensitive full-length transcriptome profiling in single cells. *Nature Methods*, *10*(11), 1096–1098. https://doi.org/10.1038/nmeth.2639

Picelli, S., Faridani, O. R., Björklund, Å. K., Winberg, G., Sagasser, S., & Sandberg, R. (2014). Full-length RNA-seq from single cells using Smart-seq2. *Nature Protocols*, *9*(1), 171–181. https://doi.org/10.1038/nprot.2014.006

Quennell, J. H., Mulligan, A. C., Tups, A., Liu, X., Phipps, S. J., Kemp, C. J., … Anderson, G. M. (2009). Leptin Indirectly Regulates Gonadotropin-Releasing Hormone Neuronal Function. *Endocrinology*, *150*(6), 2805–2812. https://doi.org/10.1210/en.2008-1693

Rahmouni, K., Morgan, D. A., Morgan, G. M., Mark, A. L., & Haynes, W. G. (2005). Role of selective leptin resistance in diet-induced obesity hypertension. *Diabetes*, *54*(7), 2012–2018. Retrieved from http://www.ncbi.nlm.nih.gov/pubmed/15983201

Robker, R. L., Wu, L. L.-Y., & Yang, X. (2011). Inflammatory pathways linking obesity and ovarian dysfunction. *Journal of Reproductive Immunology*, *88*(2), 142–148. https://doi.org/10.1016/j.jri.2011.01.008

Russell, D. L., Gilchrist, R. B., Brown, H. M., & Thompson, J. G. (2016a). Bidirectional communication between cumulus cells and the oocyte: Old hands and new players? *Theriogenology*, *86*(1), 62–68. https://doi.org/10.1016/j.theriogenology.2016.04.019

Russell, D. L., Gilchrist, R. B., Brown, H. M., & Thompson, J. G. (2016b). Bidirectional communication between cumulus cells and the oocyte: Old hands and new players? *Theriogenology*, *86*(1), 62–68. https://doi.org/10.1016/j.theriogenology.2016.04.019

Ryan, N. K., Woodhouse, C. M., Van der Hoek, K. H., Gilchrist, R. B., Armstrong, D. T., & Norman, R. J. (2002). Expression of leptin and its receptor in the murine ovary: possible role in the regulation of oocyte maturation. *Biology of Reproduction*, *66*(5), 1548–1554. Retrieved from http://www.ncbi.nlm.nih.gov/pubmed/11967222

Sahu, A. (2003). Leptin signaling in the hypothalamus: emphasis on energy homeostasis and leptin resistance. *Frontiers in Neuroendocrinology*, *24*(4), 225–253. Retrieved from http://www.ncbi.nlm.nih.gov/pubmed/14726256

Schelbert, K. B. (2009). Comorbidities of Obesity. *Primary Care: Clinics in Office Practice*, *36*(2), 271–285. https://doi.org/10.1016/J.POP.2009.01.009

Shannon, P., Markiel, A., Ozier, O., Baliga, N. S., Wang, J. T., Ramage, D., … Ideker, T. (2003). Cytoscape: A Software Environment for Integrated Models of Biomolecular Interaction Networks. *Genome Research*, *13*(11), 2498–2504. https://doi.org/10.1101/gr.1239303

Sierra-Honigmann, M. R., Nath, A. K., Murakami, C., Garcia-Cardena, G., Papapetropoulos, A., Sessa, W. C., … Flores-Riveros, J. R. (1998). Biological action of leptin as an angiogenic factor 1. *Science*, *281*(0036-8075 (Print)), 1683–1686.

Su, G., Kuchinsky, A., Morris, J. H., States, D. J., & Meng, F. (2010). GLay: community structure analysis of biological networks. *Bioinformatics*, *26*(24), 3135–3137. https://doi.org/10.1093/bioinformatics/btq596

Su, Gang, Kuchinsky, A., Morris, J. H., States, D. J., & Meng, F. (2010). GLay: community structure analysis of biological networks. *Bioinformatics (Oxford, England)*, *26*(24), 3135–3137. https://doi.org/10.1093/bioinformatics/btq596

Sugiura, K., Pendola, F. L., & Eppig, J. J. (2005). Oocyte control of metabolic cooperativity between oocytes and companion granulosa cells: energy metabolism. *Developmental Biology*, *279*(1), 20–30. https://doi.org/10.1016/j.ydbio.2004.11.027

Sutton-McDowall, M. L., Gilchrist, R. B., & Thompson, J. G. (2010). The pivotal role of glucose metabolism in determining oocyte developmental competence. *REPRODUCTION*, *139*(4), 685–695. https://doi.org/10.1530/REP-09-0345

Swain, J. E., Dunn, R. L., McConnell, D., Gonzalez-Martinez, J., & Smith, G. D. (2004). Direct Effects of Leptin on Mouse Reproductive Function: Regulation of Follicular, Oocyte, and Embryo Development. *Biology of Reproduction*, *71*(5), 1446–1452. https://doi.org/10.1095/biolreprod.104.033035

Szanto, I., & Kahn, C. R. (2000). Selective interaction between leptin and insulin signaling pathways in a hepatic cell line. *Proceedings of the National Academy of Sciences*, *97*(5), 2355–2360. https://doi.org/10.1073/pnas.050580497

Tao, W., Pennica, D., Xu, L., Kalejta, R. F., & Levine, A. J. (2001). Wrch-1, a novel member

of the Rho gene family that is regulated by Wnt-1. *Genes & Development*, *15*(14), 1796–1807. https://doi.org/10.1101/gad.894301

Tchasovnikarova, I. A., Timms, R. T., Matheson, N. J., Wals, K., Antrobus, R., Göttgens, B., … Lehner, P. J. (2015). GENE SILENCING. Epigenetic silencing by the HUSH complex mediates position-effect variegation in human cells. *Science (New York, N.Y.)*, *348*(6242), 1481–1485. https://doi.org/10.1126/science.aaa7227

Thompson, J. G., Lane, M., & Gilchrist, R. B. (2007). Metabolism of the bovine cumulus-oocyte complex and influence on subsequent developmental competence. *Society of Reproduction and Fertility Supplement*, *64*, 179–190. Retrieved from http://www.ncbi.nlm.nih.gov/pubmed/17491147

Timms, R. T., Tchasovnikarova, I. A., Antrobus, R., Dougan, G., & Lehner, P. J. (2016). ATF7IP-Mediated Stabilization of the Histone Methyltransferase SETDB1 Is Essential for Heterochromatin Formation by the HUSH Complex. *Cell Reports*, *17*(3), 653–659. https://doi.org/10.1016/j.celrep.2016.09.050

Tripal, P., Bauer, M., Naschberger, E., Mörtinger, T., Hohenadl, C., Cornali, E., … Stürzl, M. (2007). Unique Features of Different Members of the Human Guanylate-Binding Protein Family. *Journal of Interferon & Cytokine Research*, *27*(1), 44–52. https://doi.org/10.1089/jir.2007.0086

Unger, R. H., & Zhou, Y. T. (2001). Lipotoxicity of beta-cells in obesity and in other causes of fatty acid spillover. *Diabetes*, *50 Suppl 1*(suppl 1), S118-21. https://doi.org/10.2337/DIABETES.50.2007.S118

Unger, R. H., Zhou, Y. T., & Orci, L. (1999). Regulation of fatty acid homeostasis in cells: novel role of leptin. *Proceedings of the National Academy of Sciences of the United States of America*, *96*(5), 2327–2332. https://doi.org/10.1073/pnas.96.5.2327

Untergasser, A., Cutcutache, I., Koressaar, T., Ye, J., Faircloth, B. C., Remm, M., & Rozen, S. G. (2012). Primer3—new capabilities and interfaces. *Nucleic Acids Research*, *40*(15), e115–e115. https://doi.org/10.1093/nar/gks596

Uyar, A., Torrealday, S., & Seli, E. (2013). Cumulus and granulosa cell markers of oocyte and embryo quality. *Fertility and Sterility*, *99*(4), 979–997. https://doi.org/10.1016/j.fertnstert.2013.01.129

Vaisberg, E. A., Grissom, P. M., & McIntosh, J. R. (1996). Mammalian cells express three distinct dynein heavy chains that are localized to different cytoplasmic organelles. *The Journal of Cell Biology*, *133*(4), 831–842. https://doi.org/10.1083/jcb.133.4.831

Vaisse, C., Halaas, J. L., Horvath, C. M., Darnell, J. E., Stoffel, M., & Friedman, J. M. (1996). Leptin activation of Stat3 in the hypothalamus of wild–type and ob/ob mice but not db/db mice. *Nature Genetics*, *14*(1), 95–97. https://doi.org/10.1038/ng0996-95

Vanorny, D. A., & Mayo, K. E. (2017). The role of Notch signaling in the mammalian ovary. *Reproduction*, *153*(6), R187–R204. https://doi.org/10.1530/REP-16-0689

Wu, Linda L.-Y., Norman, R. J., & Robker, R. L. (2012). The impact of obesity on oocytes: evidence for lipotoxicity mechanisms. *Reproduction, Fertility and Development*, *24*(1), 29. https://doi.org/10.1071/RD11904

Wu, Linda Lin-Yan, Dunning, K. R., Yang, X., Russell, D. L., Lane, M., Norman, R. J., & Robker, R. L. (2010). High-Fat Diet Causes Lipotoxicity Responses in Cumulus–Oocyte Complexes and Decreased Fertilization Rates. *Endocrinology*, *151*(11), 5438–5445. https://doi.org/10.1210/en.2010-0551

Yamagishi, S., Edelstein, D., Du, X., Kaneda, Y., Guzmán, M., & Brownlee, M. (2001). Leptin Induces Mitochondrial Superoxide Production and Monocyte Chemoattractant Protein-1 Expression in Aortic Endothelial Cells by Increasing Fatty Acid Oxidation via Protein Kinase A. *Journal of Biological Chemistry*, *276*(27), 25096–25100. https://doi.org/10.1074/jbc.M007383200

Zabolotny, J. M., Bence-Hanulec, K. K., Stricker-Krongrad, A., Haj, F., Wang, Y., Minokoshi,

Y., … Neel, B. G. (2002). PTP1B regulates leptin signal transduction in vivo. *Developmental Cell*, *2*(4), 489–495. Retrieved from http://www.ncbi.nlm.nih.gov/pubmed/11970898

Zhao, S., & Fernald, R. D. (2005). Comprehensive Algorithm for Quantitative Real-Time Polymerase Chain Reaction. *Journal of Computational Biology*, *12*(8), 1047–1064. https://doi.org/10.1089/cmb.2005.12.1047

Figure 1. Wołodko et al. 2019

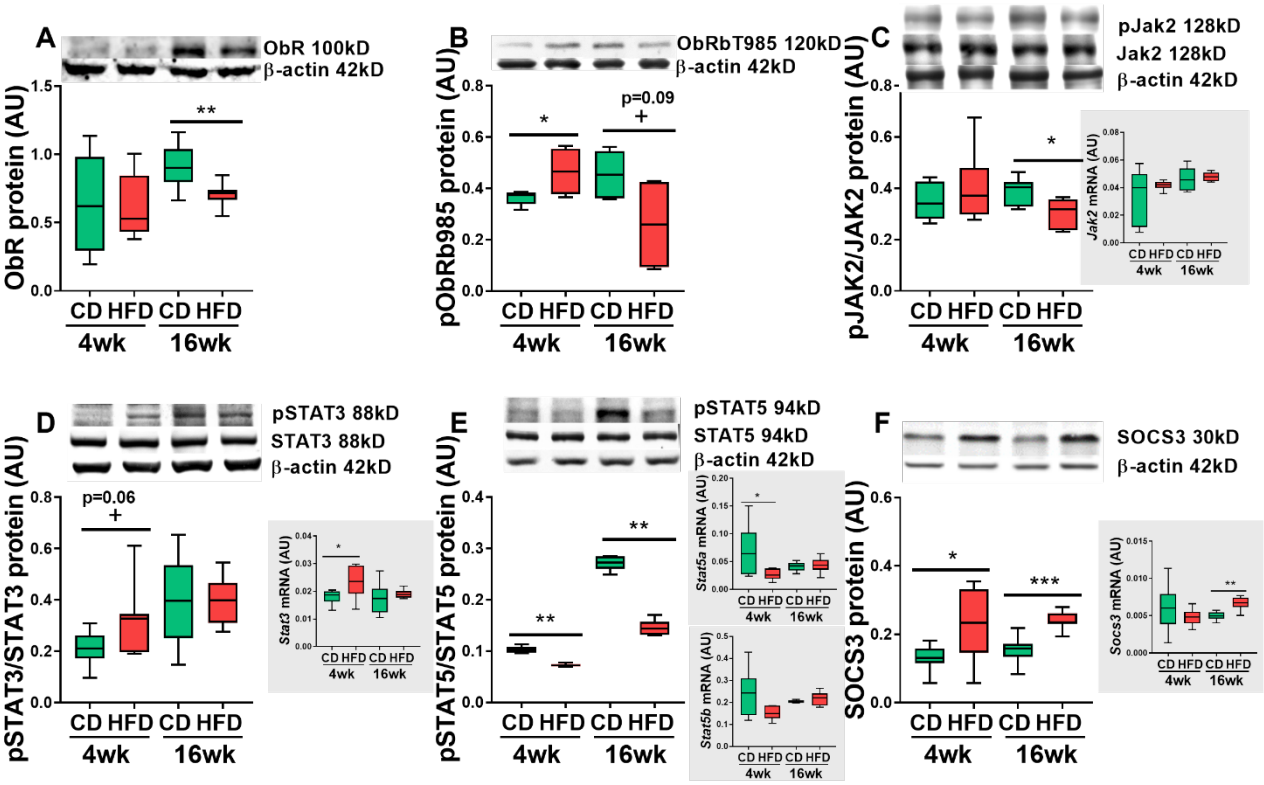

Figure 1 The establishment of leptin resistance in the ovary of diet induced obese mice confirmed with decreased ObRb-pTyr985 and pJAK2 and increased SOCS3 protein.

Transcript and protein abundance of components of the leptin signalling pathway in ovarian extracts. Animals were maintained on chow diet (CD) or high fat diet (HFD) for 4 weeks (wk) or 16 weeks. Expression of (A) ObR protein, (B) phosphorylation of tyrosine 985 of leptin receptor, (C) *Jak2* mRNA (grey box) and phosphorylation of Jak2, (D) *Stat3* mRNA (grey box) and phosphorylation of STAT3, (E) *Stat5a/b* mRNA (grey box) and phosphorylation of STAT5, (F) *Socs3* mRNA (grey box) and protein SOCS3. mRNA expression of *Rpl32* and protein expression of β-actin were used to normalize the expression data. Each bar represents the mean +/- SD. Differences between groups were analyzed by Mann-Whitney test. N=4-8 for immunoblots and N=8 for RT-PCR analysis. * $p<0.05$; ** $p<0.01$; ***$p<0.001$.

The following supplementary files and figure supplements are available for figure 1:

Supplementary file 1 Table 1. This file contains primer sequences used for quantitative real time PCR

Supplementary file 2 Table 2. This file contains specification of antibodies used for Western Blotting

Figure 1- figure supplement 1. Expression of leptin signalling components in the ovary of diet induced obese mice.

Figure 1- figure supplement 2. Phenotype characterisation of diet-induced obese mice

Figure 2. Wołodko et al. 2019

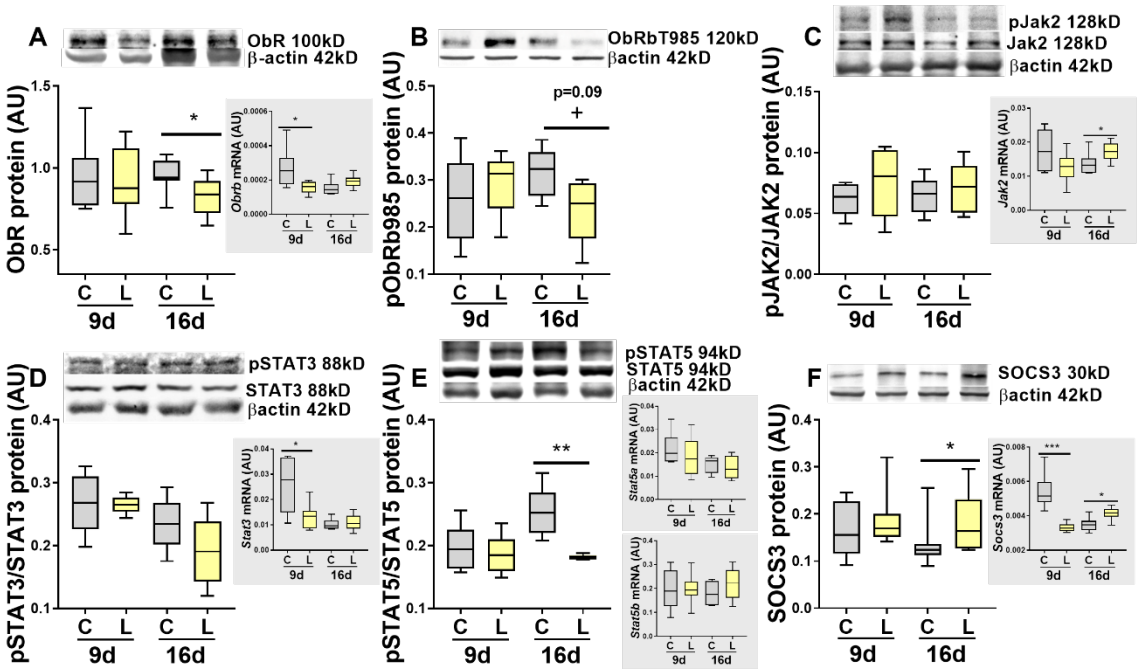

Figure 2 Pharmacologically hyperleptinemic mice model validation.

Transcript and protein abundance of components of the leptin signalling pathway in ovarian extracts. Animals were injected with saline (C) or leptin (L) for 9 or 16 days (d). Expression of (A) *ObRb* mRNA (grey box) and ObR protein, (B) phosphorylation of tyrosine 985 of leptin receptor, (C) *Jak2* mRNA (grey box) and phosphorylation of JAK2, (D) *Stat3* mRNA (grey box) and phosphorylation of STAT3, (E) *Stat5a/b* mRNA (grey box) and phosphorylation of STAT5, (F) *Socs3* mRNA (grey box) and protein SOCS3. mRNA abundance of *Rpl32* and protein abundance of β-actin was used to normalize the expression data. Each bar represents the mean +/- SD. Differences between groups were analyzed by Mann- Whitney test. N=4-8 for immunoblots and N=8 for RT-PCR analysis. * $p<0.05$; ** $p<0.01$; ***$p<0.001$.

The following supplementary files and figure supplements are available for figure 2:

Supplementary file 1 Table 1. This file contains primer sequences used for quantitative real time PCR

Supplementary file 2 Table 2. This file contains specification of antibodies used for Western Blotting

Figure 2- figure supplement 1. Expression of leptin signalling components in the ovary of pharmacologically hyperleptinemic mice.

Figure 2- figure supplement 2. Phenotype characterisation of pharmacologically hyperleptinemic mice

Figure 2- figure supplement 3 - Phenotype characterisation of leptin and leptin receptor deficient mice

Figure 2- figure supplement 4 - Plasma level of adipokines and insulin, and SOCS3 concentration in ovary extracts of diet-induced obeseand pharmacological hyperleptinemic mice.

Figure 3. Wołodko et al. 2019

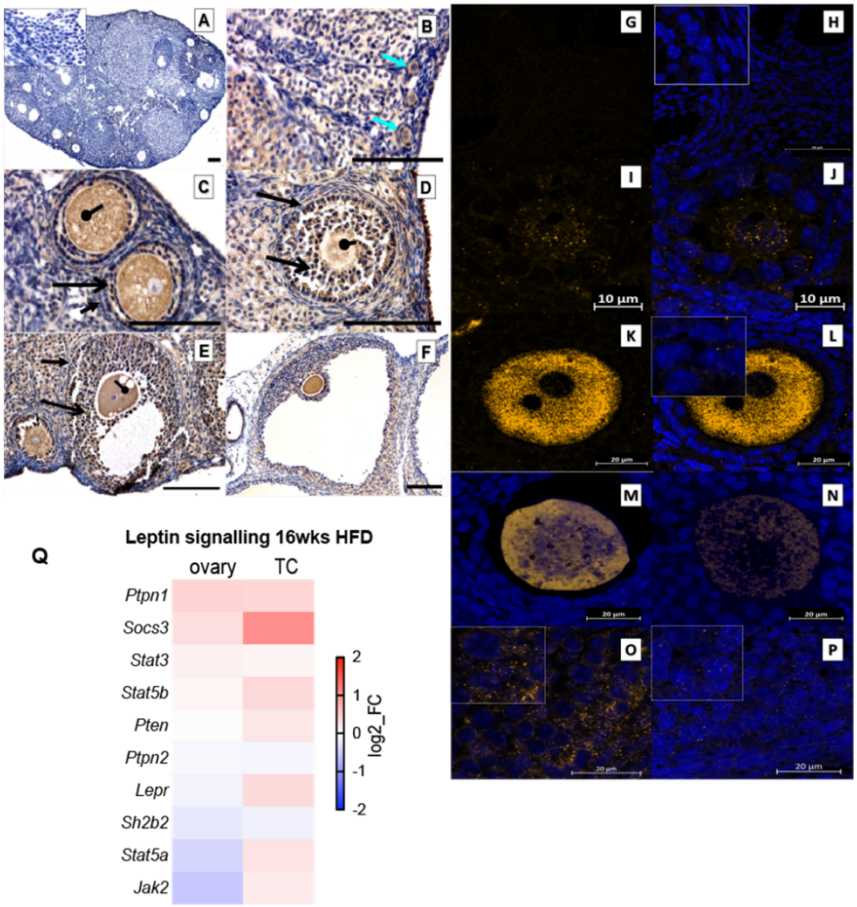

Figure 3 SOCS3 - Expression in different ovarian compartments.

Immunohistochemical localisation of SOCS3 protein during follicle development in ovaries of mice treated with leptin (LEPT), subjected to diet-induced obesity (4wk and 16wk HFD), or corresponding CD controls. Positive staining in brown, counterstaining with heamatoxylin. Images randomly assigned between DIO and LEPT: (A) negative control performed with polyclonal rabbit IgG 4wk CD; SOCS3 is detected in (B) primordial follicles 4wk CD, (C) primary follicles 4wk CD, (D) secondary follicles 16 wk HFD, (E) antral follicle 16 wk HFD and (F) preovulatory follicle LEPT. Staining is present in oocyte, granulosa and theca cells. Bright blue arrows depicts primordial follicles; oval shape arrow depicts oocyte, black arrow depicts granulosa cells and arrow depicts theca cells. Scale bars represent 100µm. The staining was confirmed by immunofluorescent localisation of SOCS3. Positive staining in orange, nuclear counterstaining with DAPI in blue. (G-H) negative control 16 wk CD performed with polyclonal rabbit IgG, SOCS3 localised in (I-J) primordial follicles 16 wk CD, (K-L) primary follicles 16 wk CD. SOCS3 expression in ovaries from leptin deficient ovaries in secondary follicle (M, N) and antral follicle (O,P) from heterozygous controls (*ob/ob.* +/+; M,O) and homozygotes (*ob/ob* -/-; N,P). Images are representatives of >3 biological replicates. Inserts in left top corner are the amplifications of granulosa cells. (Q) Heatmap showing fold of change in expression of mRNA of leptin signalling components measured in whole ovary or theca cells (TC) by RT-PCR. *Rpl32* mRNA expression was used to normalize the expression data. N=8.

The following figure supplement is available for figure 3:

Figure 3- figure supplement 1 – Immunolocalisation of SOCS3 and PTP1B protein in the mouse ovary.

Figure 4. Wołodko et al. 2019

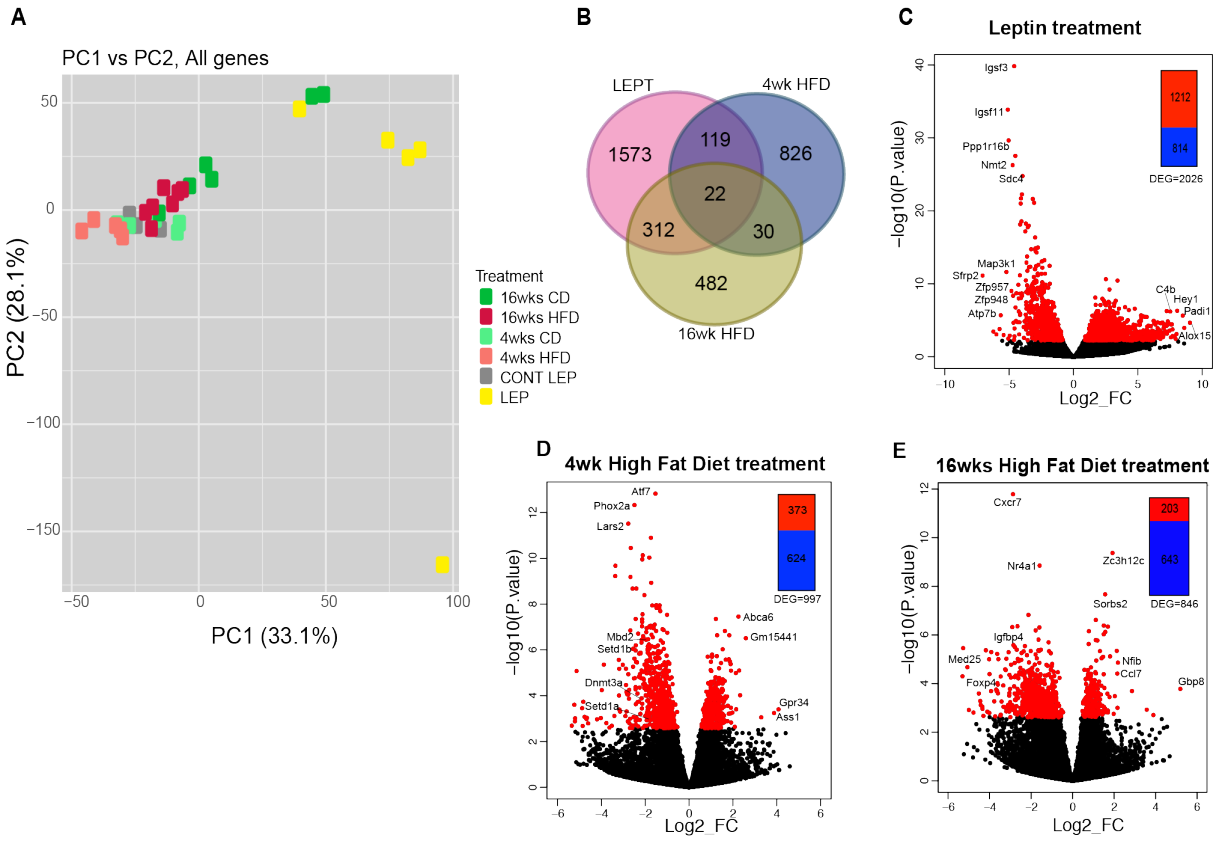

Figure 4 - Cumulus cell transcriptome analysis: leptin vs. diet induced-obesity.

RNA-Seq analysis of gene expression in cumulus cells obtained from mice treated with saline (CONT) and leptin (LEPT) or after 4 or 16 weeks (wk) of chow diet (CD) or high fat diet (HFD). N= 3-7 mice per group. (A) Principal component analysis of global transcriptome shows LEPT effect is the main source of variance in the data (first principal component, PC1). (B) Venn diagram showing the number of genes differentially expressed at false discovery rate (FDR) <0.05 between LEPT, 4wk HFD and 16wk HFD group. Volcano plots showing distribution of differentially expressed genes in (C) LEPT group, (D) 4wks HFD and (E) 16wks HFD. log2_FC of reads per million (RPM)

The following supplementary files and figure supplements are available for figure 4:

Supplementary file 3 Table 3. This file contains list of genes and associated pathways upregulated and downregulated in cumulus cells from hyperleptinemic mice.

Supplementary file 4 Table 4. This file contains list of genes and associated pathways upregulated and downregulated in cumulus cells from mice after 4 weeks of diet-induced obesity

Supplementary file 5 Table 5. This file contains list of genes and associated pathways upregulated and downregulated in cumulus cells from mice after 16 weeks of diet-induced obesity

Figure 4- figure supplement 1 - Differentially expressed genes and associated pathways in cumulus cells from LEPT and DIO protocols.

Figure 5. Wołodko et al. 2019

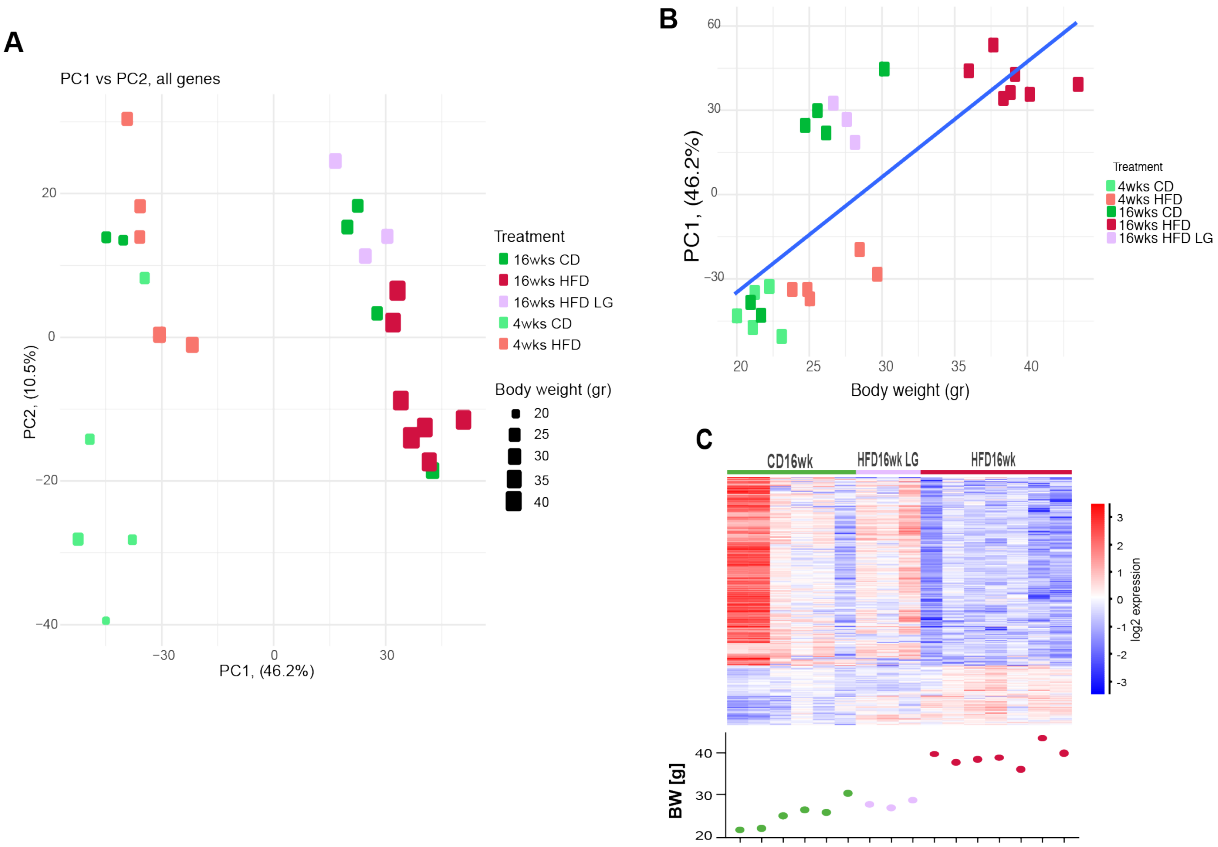

Figure 5 - Correlation of cumulus cell transcriptome with body mass.

RNA-Seq analysis of gene expression in cumulus cells obtained from mice after 4 or 16 weeks (wk), chow diet (CD), high fat diet (HFD) or low gainers on HFD (HFDLG). N= 3-7 mice per group. (A) Principal component analysis of global transcriptome showing samples distrubution. (B) Plot showing correlation of Principal Component 1 with body weight r=0.777; (p=3.026e-06). (C) DESeq2 analysis of transcriptome data, heatmap representing fold of change of gene expression between different groups.

The following supplementary files and figure supplements are available for figure 4:

Supplementary file 6 Table 6. This file contains read counts and body weight values in cumulus cells samples from diet-induced obese and hyperleptinemic mice.

Supplementary file 7 Table 7. This file contains list of genes differently expressed in cumulus cells from diet-induced obese and hyperleptinemic mice.

Supplementary file 8 Table 8. This file contains list of genes, principal component 1 (PC1) values and correlation values in cumulus cells after analysis of correlation between PC1 and body weight.

Figure 6. Wołodko et al. 2019

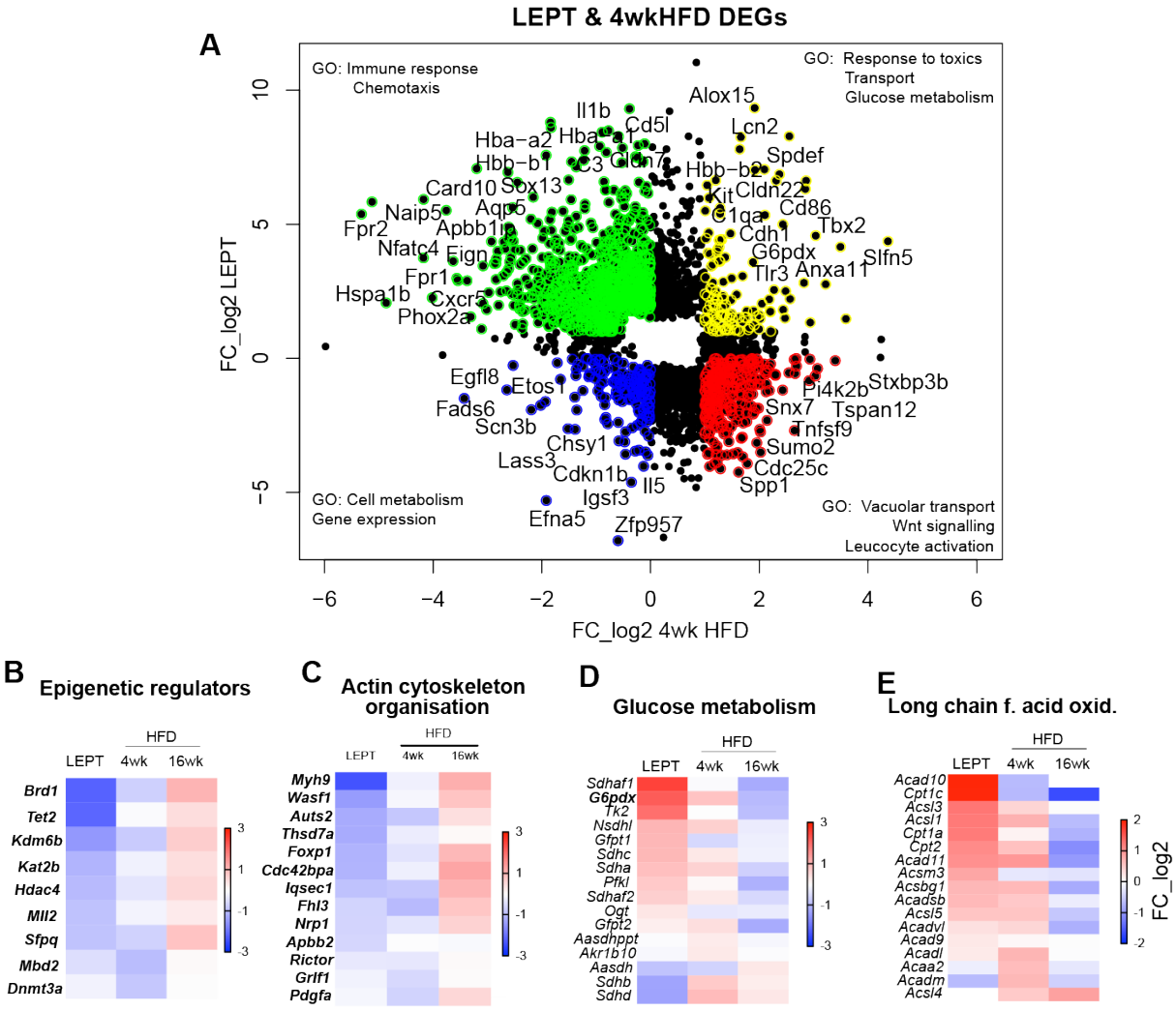

Figure 6 Similarities between profiles of genes differentially expressed in cumulus cells in diet induced-obese mice and leptin-treated mice.

DESeq2 analysis of transcriptome data in cumulus cells (CC) obtained from mice treated with saline (CONT) and leptin (LEPT) or after 4 or 16 weeks (wk) of chow diet (CD) or high fat diet (HFD). N= 3-7 mice per group. (A) Scatter plot presents overlapping genes differentially expressed in cumulus cells in LEPT and 4wk HFD (in bold genes with FDR <0.05) after DESeq2 analysis. Heatmaps presenting fold change in expression of genes associated with following pathways: (B) epigenetic regulations, (C) actin cytoskeleton organisation, (D) glucose metabolism, (E) long chain fatty acid oxidation in CC. Gene onthology analysis performed with Gene Ontology Enrichment Analysis and Visualisation Tool. log2_FC of reads per million (RPM)

The following supplementary file and figure supplement are available for figure 6:

Supplementary file 9 Table 9. This file contains list of common genes and associated pathways upregulated and downregulated in cumulus cells from hyperleptinemic mice and from mice after 4 weeks of diet-induced obesity.

Figure 6- figure supplement 1 - Similarities between profiles of genes differentially expressed in cumulus cells in diet induced- obese mice and leptin treated mice.

Figure 7. Wołodko et al. 2019

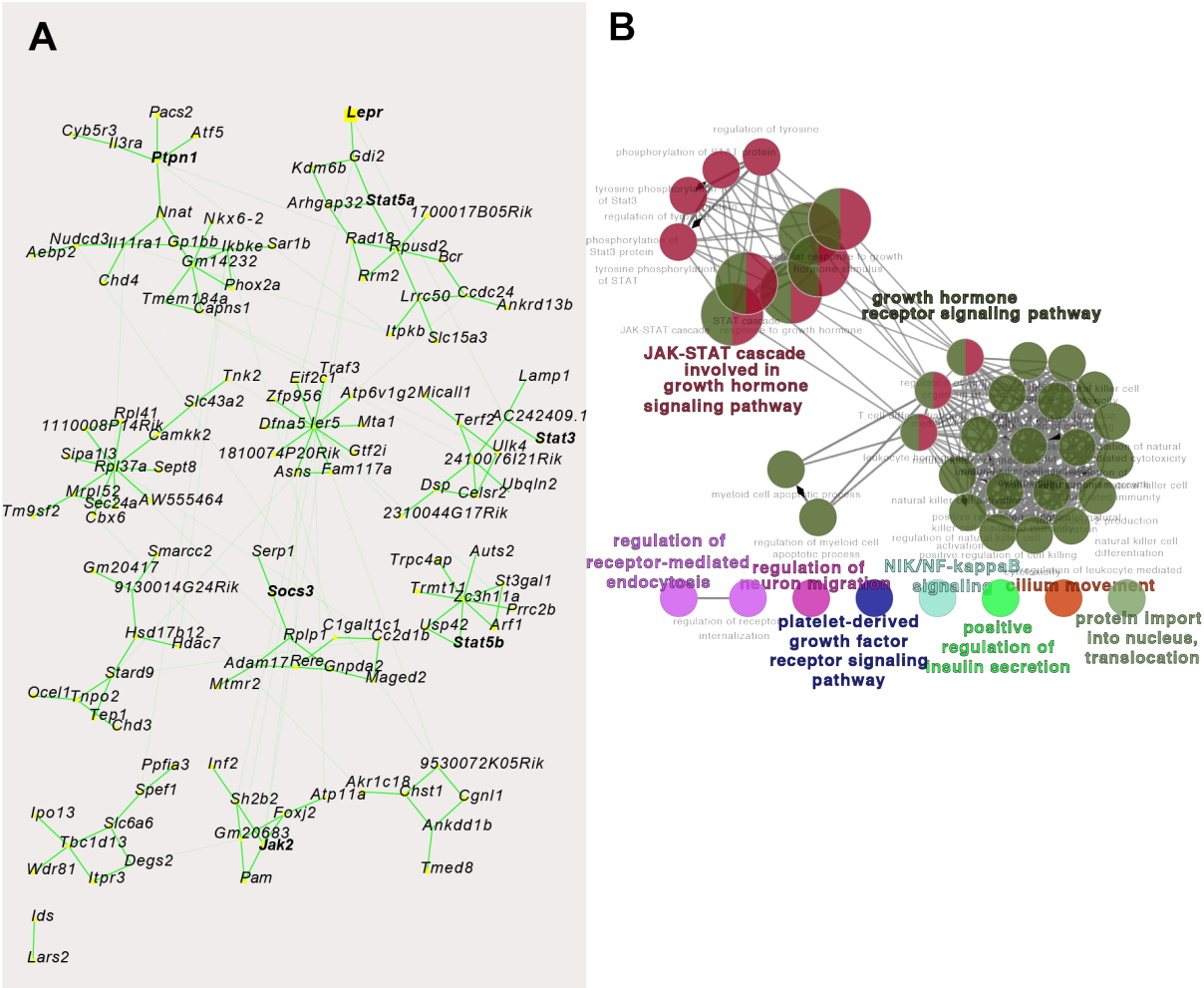

Figure 7 - Network revealing interactions between leptin signalling components and DEGs for LEPT and 4 wk DIO. A co-expression network was constructed using the pairwise correlations (r > 0.9) between genes of the leptin signalling pathway and DEGs for LEPT and 4 wk DIO. The network was partitioned into clusters using Glay community clustering, which identified 12 clusters (A). The network was also subjected to biological function enrichment using using ClueGo (B).

The following supplementary file is available for figure 7:

Supplementary file 10 Table 10. This file contains list of pathways associated with the clusters described for the DEGs in cumulus cells from LEPT and 4 wk DIO.

Figure 8. Wołodko et al. 2019

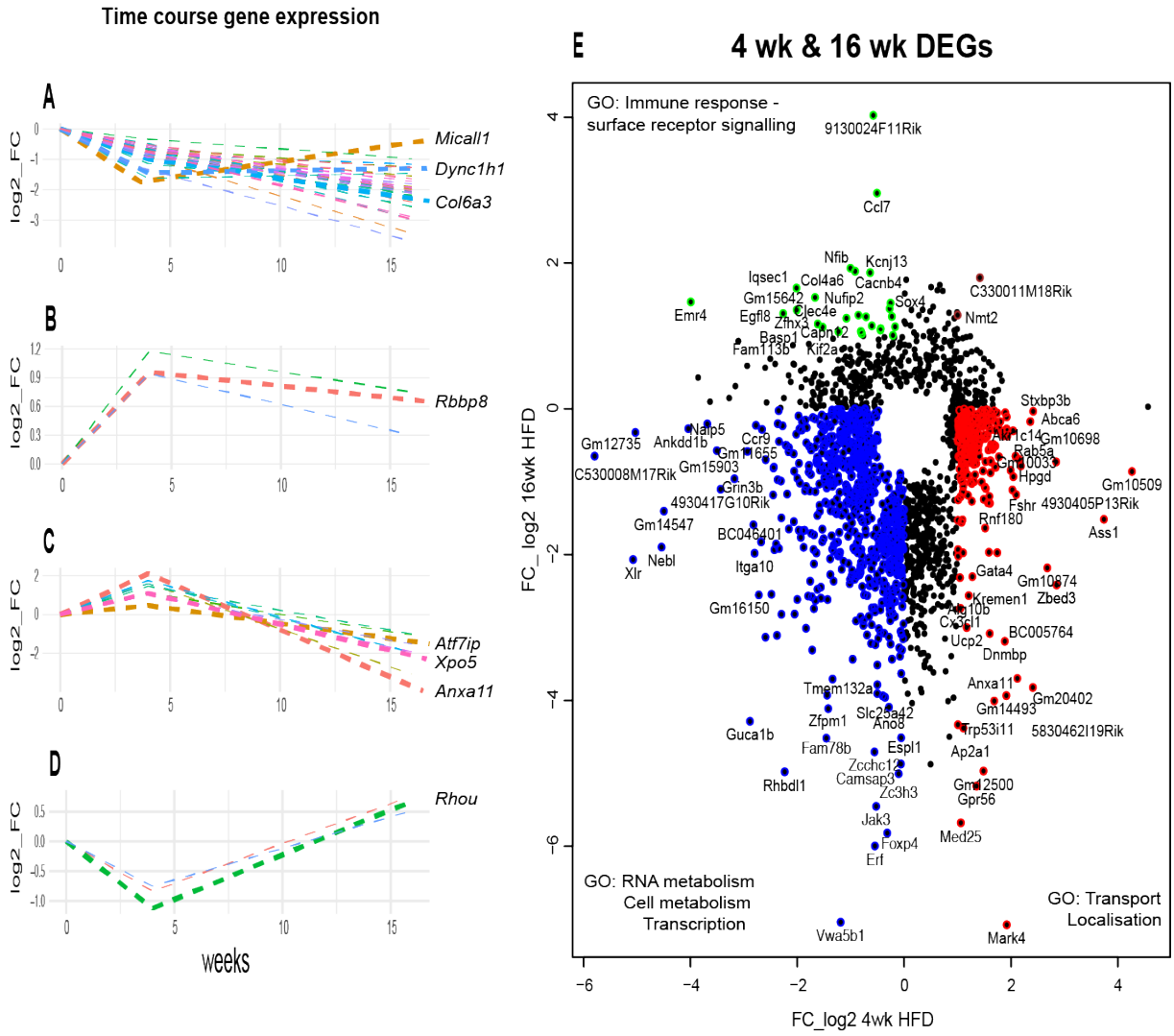

Figure 8 - Time course analysis of changes in the cumulus cell transcriptome during obesity progression. DESeq2 analysis of transcriptome data in cumulus cells (CC) for the timepoints 0, 4 or 16 weeks (wk) of chow diet (CD) or high fat diet (HFD) fed mice. N= 3-7 mice per group. Line graphs present profiles of gene expression for genes significantly changed in both 4 and 16wk. (A) genes downregulated after 4wk and 16wk HFD, (B) genes upregulated after 4wk and 16wk HFD, (C) genes upregulated after 4wk and downregulated after 16wk HFD, (D) genes downregulated after 4wk and upregulated after 16wk HFD. (E) Scatter plot presents overlapping genes differentially expressed in at least one condition (FDR <0.05) in CC after 4wk and 16wk HFD. Gene ontology analysis performed with Gene Onthology Enrichment Analysis and Visualisation Tool. log2_FC of reads per million (RPM)

The following supplementary file is available for figure 8:

Supplementary file 11 Table 11. This file contains list of common genes and associated pathways upregulated and downregulated in cumulus cells from mice after 4 and 16 weeks of diet-induced obesity.

Figure 9. Wołodko et al. 2019

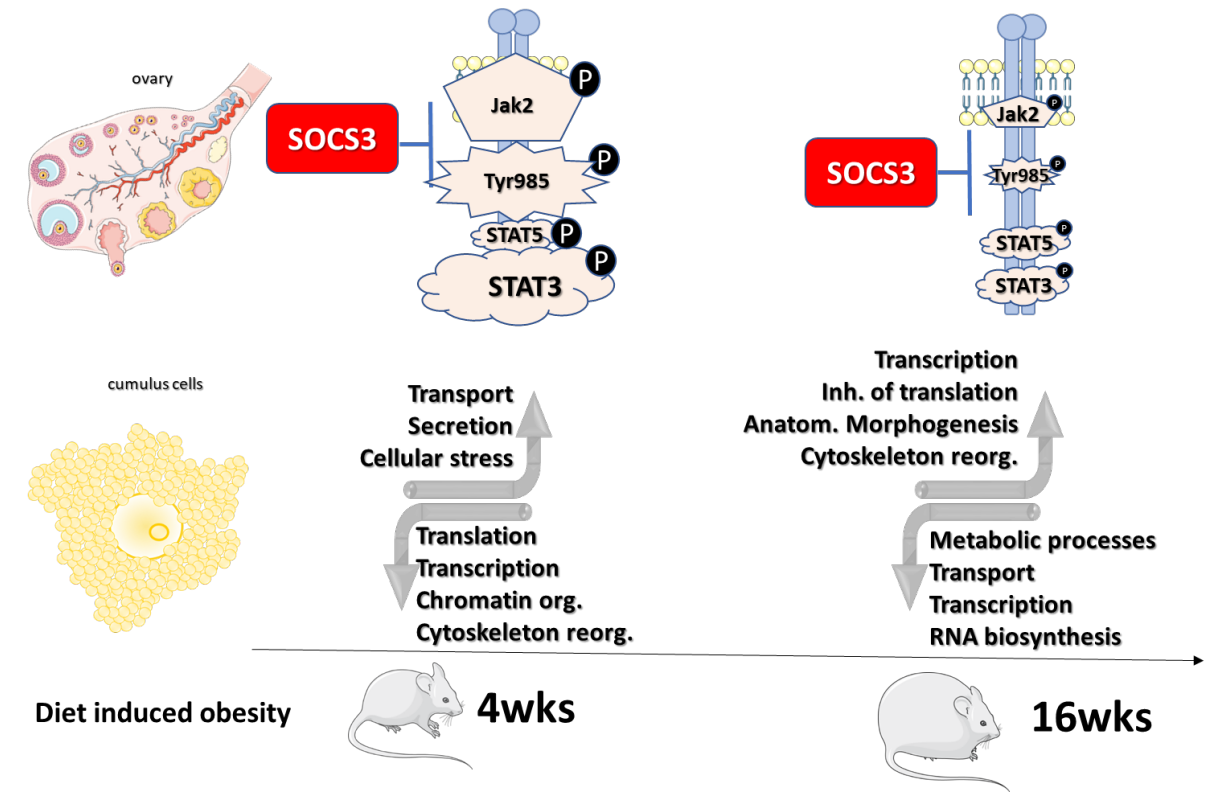

Figure 9 - Graphical abstract of the main findings.
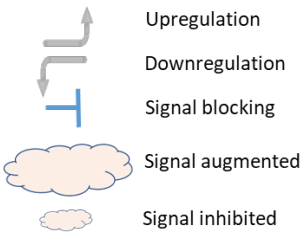
In the ovary: Using diet-induced obesity (DIO) model showing the time-course impairment of leptin signalling in the ovary and major changes in cumulus cells (CC). After 4 weeks (wks) DIO, leptin signalling was upregulated through increased phosphorylation (p) of Tyr985 of leptin receptor, pSTAT3 and SOCS3 expression, alongside decreased pSTAT5. After 16 wks DIO, decreased pJAK2, pTyr985, pSTAT5, paralleled by SOCS3 upregulation confirms establishment of leptin resistance. In CCs: transcriptome analysis showing pathways up and downregulated during obesity: early changes (4wks) mainly comprise alterations of membrane trafficking, cytoskeleton organisation and inhibition of gene expression and epigenetic regulation; late changes (16wks) comprise stimulation of the inflammatory response and cell anatomical morphogenesis, with inhibition of metabolism and transport.